2020-09-08

BCL11A enhancer edited hematopoietic stem cells persist in rhesus monkeys without toxicity

Selami Demirci
National Institutes of Health

Et al.

JCI The Journal of Clinical Investigation

BCL11A enhancer edited hematopoietic stem cells persist in rhesus monkeys without toxicity

Selami Demirci, … , Daniel E. Bauer, John F. Tisdale

J Clin Invest. 2020. https://doi.org/10.1172/JCI140189.

Research In-Press Preview Hematology Transplantation

Graphical abstract

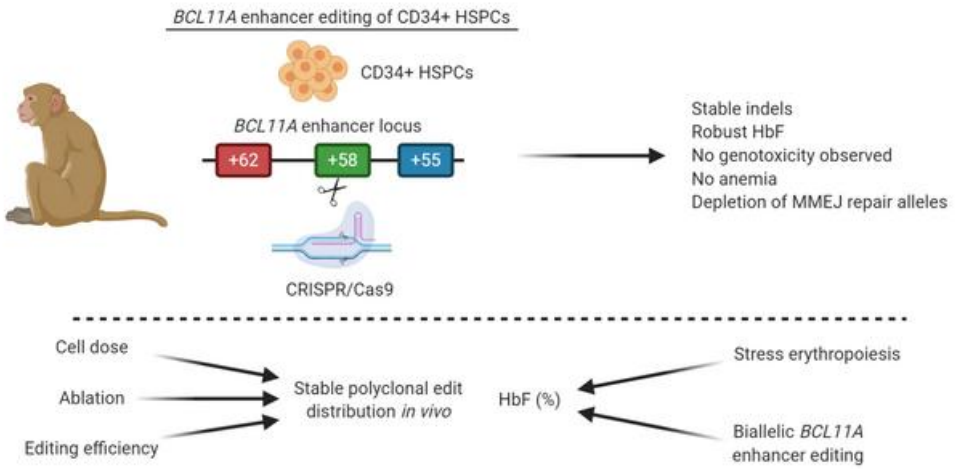

BCL11A enhancer edited hematopoietic stem cells persist in rhesus monkeys without toxicity

Selami Demirci[1#], Jing Zeng[2#], Yuxuan Wu[2,3], Naoya Uchida[1], Anne H. Shen[2], Danilo Pellin[4], Jackson Gamer[1], Morgan Yapundich[1], Claire Drysdale[1], Jasmine Bonanno[2], Aylin C. Bonifacino[5], Allen E. Krouse[5], Nathaniel S. Linde[5], Theresa Engels[5], Robert E. Donahue[1], Juan J. Haro-Mora[1], Alexis Leonard[1], Tina Nassehi[1], Kevin Luk[6], Shaina N. Porter[7], Cicera R. Lazzarotto[8], Shengdar Q. Tsai[8], Mitchell J. Weiss[8], Shondra M. Pruett-Miller[7], Scot A. Wolfe[6], Daniel E. Bauer[2], and John F. Tisdale[1*]

1) Cellular and Molecular Therapeutics Branch, National Heart Lung and Blood Institutes (NHLBI) / National Institute of Diabetes and Digestive and Kidney Diseases (NIDDK), National Institutes of Health (NIH), Bethesda, MD, USA

2) Division of Hematology/Oncology, Boston Children's Hospital, Department of Pediatric Oncology, Dana-Farber Cancer Institute, Department of Pediatrics, Harvard Stem Cell Institute, Broad Institute, Harvard Medical School, Boston, MA, USA.

3) Shanghai Key Laboratory of Regulatory Biology, Institute of Biomedical Sciences and School of Life Sciences, East China Normal University, Shanghai, China.

4) Gene Therapy Program, Dana-Farber/Boston Children's Cancer and Blood Disorders Center, Harvard Medical School, Boston, MA, USA.

5) Translational Stem Cell Biology Branch, NHLBI, NIH, Bethesda, MD, USA

6) Department of Molecular, Cell and Cancer Biology, Li Weibo Institute for Rare Diseases Research, University of Massachusetts Medical School, Worcester, MA, USA

7) Department of Cell and Molecular Biology, Center for Advanced Genome Engineering, St. Jude Children's Research Hospital, Memphis, TN, USA

8) Department of Hematology, St. Jude Children's Research Hospital, Memphis, TN, USA.

[#] Equally contributed

Competing interests

The authors have declared that no conflict of interest exists.

Corresponding author; John F. Tisdale, Cellular and Molecular Therapeutics Branch, National Heart Lung and Blood Institutes (NHLBI)/National Institute of Diabetes and Digestive and Kidney Diseases (NIDDK), NIH, 9000 Rockville Pike, Bldg. 10,9N112, Bethesda, MD 20892, USA. **e-mail**: johntis@mail.nih.gov

Abstract

Gene editing of the erythroid-specific *BCL11A* enhancer in hematopoietic stem and progenitor cells (HSPCs) from sickle cell disease (SCD) patients induces fetal hemoglobin (HbF) without detectable toxicity as assessed by mouse xenotransplant. Here, we evaluated autologous engraftment and HbF induction potential of erythroid-specific *BCL11A* enhancer edited HSPCs in four non-human primates. We utilized a single guide RNA (sgRNA) with identical human and rhesus target sequences to disrupt a GATA1 binding site at the *BCL11A* +58 erythroid enhancer. Cas9 protein and sgRNA ribonucleoprotein complex (RNP) was electroporated into rhesus HSPCs, followed by autologous infusion after myeloablation. We found that gene edits persisted in peripheral blood (PB) and bone marrow (BM) for up to 101 weeks similarly for *BCL11A* enhancer or control locus (*AAVS1*) targeted cells. Biallelic *BCL11A* enhancer editing resulted in robust γ-globin induction, with the highest levels observed during stress erythropoiesis. Indels were evenly distributed across PB and BM lineages. Off-target edits were not observed. Non-homologous end-joining repair alleles were enriched in engrafting HSCs. In summary, we find that edited HSCs can persist for at least 101 weeks post-transplant and biallelic edited HSCs provide substantial HbF levels in PB red blood cells, together supporting further clinical translation of this approach.

Keywords: Sickle cell disease, β-thalassemia, γ-globin, CRISPR/Cas9, gene editing

Introduction

The β-hemoglobin (*HBB*) disorders, including sickle cell disease (SCD) and β-thalassemia, are the most common single-gene inherited disorders, resulting in severe morbidity and mortality worldwide. The only curative therapeutic modality for these conditions is allogeneic hematopoietic stem cell transplantation (HSCT), which is limited by a shortage of matched donors (1) and may be associated with graft-versus-host disease. Induction of fetal hemoglobin (HbF) in adults with SCD has proven clinically beneficial for patients with severe disease because γ-globin inhibits hemoglobin (Hb) polymerization under deoxygenated conditions by incorporating into tetramers and decreasing sickle hemoglobin (HbS) concentration in red blood cells (RBCs) (2). In addition, a high level of HbF in β-thalassemia patients is associated with amelioration of disease severity as γ-globin improves α/β-chain imbalance and HbF replaces deficient adult hemoglobin (HbA) (3). Genome-wide association studies recognized *BCL11A* as a significant repressor of γ-globin expression (4, 5), and multiple lines of evidence have validated its negative regulatory activity (6, 7). In addition to its HbF silencing role, *BCL11A* is required for normal B-cell development and hematopoietic stem cell (HSC) function. We and others previously identified the intronic erythroid-specific *BCL11A* enhancer, itself subject to HbF-associated common genetic variation, as a favorable therapeutic target (8-12). We recently demonstrated that CRISPR-Cas9 disruption of the enhancer by indels (insertions and deletions introduced to the genome by DNA repair after targeted cleavage) induces HbF, inhibiting sickling and restoring globin chain balance in erythroid cells derived from hematopoietic stem and progenitor cells (HSPCs) from SCD and β-thalassemia patients respectively, without detectable genotoxicity or adverse effects on HSC function (12). Xenotransplantation of HSCs may not fully evaluate the self-renewal and peripheral blood (PB) repopulation potential required for an effective cellular therapy. In particular, xenotransplant assays may emphasize the function of progenitors over HSCs and do not support normal PB reconstitution. Since HbF is a recent evolutionary adaptation originating in a shared ancestor of humans and old-world non-

human primates, its endogenous regulation cannot be modeled easily in non-primate cells. Therefore, non-human primate autologous hematopoietic cell transplantation may be a powerful experimental system where various gene manipulations may be investigated for their feasibility, safety, and efficacy, facilitating successful clinical development (13-15). To more fully investigate the clinical potential of autologous HSC gene editing, here we evaluated engraftment and HbF induction potential of erythroid-specific *BCL11A* enhancer editing using a non-human primate transplantation model (*Rhesus macaque*) in which Hb switching is conserved (16). Advantages of the rhesus macaque autologous HSC transplant (HSCT) model include similarities between rhesus macaques and humans in genomic profile, hematopoiesis, and erythropoiesis, as well as the possibility of measuring indels and HbF in PB and bone marrow (BM) for extended time periods (17-19).

Results

Editing the BCL11A erythroid enhancer in rhesus CD34+ HSPCs induces γ-globin

We previously employed pooled sgRNA screening in human erythroid precursors to identify a core GATA1 binding site in the *BCL11A* +58 DNAse I hypersensitive site that is required for γ-globin repression (9). Subsequently, we observed that electroporation of a nuclear localization signal (NLS) sequence modified form of SpCas9 (3×NLS-SpCas9) and chemically modified synthetic guide RNA #1617 producing cleavage directly within the GATA1 binding motif produced highly efficient indels that disrupted erythroid *BCL11A* expression and prevented HbF silencing in healthy donor and β-hemoglobinopathy patient cells without detectable genotoxicity or impairment of HSC function under xenotransplantation conditions (12). The protospacer and protospacer adjacent motif (PAM) sequences are identical at the human and rhesus #1617 target sequences within the *BCL11A* +58 enhancer. Since we began these rhesus studies before identifying 3×NLS-SpCas9 as a highly efficient RNP complex for HSPC editing, in our preliminary studies we delivered 2×NLS-SpCas9:sgRNA RNP to rhesus CD34+ HSPCs by electroporation. We observed efficient editing at the *BCL11A* enhancer (using sgRNA #1617), with 81-85% indels, and at a control locus *AAVS1*, with 89-96% indels (**Figures 1A, 1B**). Following erythroid differentiation of rhesus CD34+ HSPCs, substantial γ-globin RNA induction was detected with *BCL11A* enhancer editing, with 51-83% γ-globin in *BCL11A* enhancer edited cells compared to 27-49% and 11-33% in non-electroporated and *AAVS1* control locus edited cells, respectively ($P < 0.01$, **Figure 1C**). Consistent with the RNA profiles, elevated γ-globin protein levels (54-77%, $P < 0.01$) were observed in *BCL11A* edited cells compared to non-electroporated (19-25%) and *AAVS1* edited cells (15-24%), respectively (**Figure 1D, Supplemental Figure 1A**), indicating that *BCL11A* enhancer editing de-represses HbF expression in rhesus erythroid cells. No significant difference in RBC enucleation efficiency (44-47%) following erythrocyte differentiation and viability in electroporated cells (56-68%) was observed between groups (**Supplemental Figure 1B, 1C**). Furthermore, the colony-forming unit

(CFU) capacity of the cells was comparable between the *BCL11A* edited and control groups (**Supplemental Figure 1D)**.

To test the editing frequency in HSC and progenitor fractions, we sorted CD34+CD38-CD90+CD45RA- (HSC-enriched population) and CD34+CD38+ (committed progenitors, HPCs) from CD34+ HSPCs 2 hours after RNP electroporation. Indel sequence analysis of 5-day cultured fractions revealed modestly reduced editing frequency in the HSC-enriched population (56%) compared to HPCs (72%) (**Supplemental Figure 2)**. In addition, the 15-bp deletion, a predicted microhomology-mediated end joining (MMEJ) product (20), was particularly reduced in the HSC-enriched population as compared to HPCs (from 8% to 2%) while the predominant non-homologous end-joining (NHEJ) repair product, a +1 insertion, was similar in the two populations (33% and 34%, **Supplemental Figure 2**).

Edited HSPCs produce long-term engraftment in rhesus macaques

To assess engraftment and HbF induction potential of *BCL11A* enhancer editing, we used two cohorts of macaques, with two animals per cohort. In cohort 1, we performed competitive engraftment of *BCL11A* enhancer and *AAVS1* edited CD34+ HSPCs to test the feasibility of the approach and long-term reconstitution of edited cells. Mobilized rhesus CD34+ HSPCs were electroporated with RNP composed of 2×NLS SpCas9 protein and either *BCL11A* enhancer targeting (#1617) or *AAVS1* targeting sgRNA, followed by ex vivo culture for 48 h. Cells were harvested and freshly infused into rhesus monkeys following preparative conditioning with 2×5 Gy total body irradiation (**Figure 1A**). Using a small aliquot of cells reserved for ex vivo studies, marked induction in γ-globin protein level was observed in *BCL11A* edited erythroid cells (33-45%) compared to control groups (12-27%) as determined by reverse-phase high-pressure liquid chromatography (RP-HPLC) and Hb electrophoresis, without a significant change in cell numbers among the *BCL11A* enhancer and *AAVS1* edited groups (**Supplemental Figure 3A-F**).

After CD34+ HSPC infusion (n = 2, ZL25 and ZL22, 1.23-1.42×10^6 CD34+ HSPCs/kg) (**Table 1**), animals engrafted with typical autologous reconstitution kinetics, *i.e.* 2-3 weeks as evidenced by blood cell counts and Hb levels in PB (**Supplemental Figure 4**). There was a moderate reduction in indel frequencies over the first 12 weeks after transplantation (3-15%) compared to indels in the input cell product (17-44%). However, after 12 weeks, stable indel frequencies were detected for both *BCL11A* enhancer (~3-6%) and *AAVS1* (~7-11%) in PB-derived granulocyte and lymphocyte fractions of the edited animals (**Figure 1E, 1F**, **Supplemental Figure 5A, 5B**). Stable *AAVS1* and *BCL11A* enhancer editing frequencies were found in ZL22 and ZL25 for up to 101 weeks (**Supplemental Figure 5C, 5D**) suggesting the absence of selective difference between *BCL11A* enhancer edited, *AAVS1* edited, and non-edited HSCs. Overall, these results appear consistent with previous observations that after ex vivo HSPC gene editing, indel frequencies in short-term engrafting progenitors often exceed those found in long-term engrafting HSCs (12, 21, 22).

By performing sequence analysis on individual BM mononuclear cell (MNC)-derived hematopoietic colonies, we found the *BCL11A* enhancer indels in ZL22 were distributed as ~2/3 in biallelic and ~1/3 in monoallelic edited colonies, whereas in ZL25 the *BCL11A* enhancer indels were distributed as ~15% biallelic and ~85% monoallelic edited colonies (**Figure 1G**). Blood cell counts returned to the normal range after autologous reconstitution (**Supplemental Figure 4**). In addition, gene editing did not change the frequency or distribution of BM MNC-derived colonies from ZL25 and ZL22 as compared to an unedited control animal (**Supplemental Figure 5E-G**).

To analyze γ-globin induction in edited animals, we performed RP-HPLC from PB over time. There was a substantial induction of γ-globin during the first 12 weeks post-transplantation (4.3-14.6%) that gradually decreased and stabilized at pre-transplantation levels (~0.5%) by around 20 weeks post-transplantation (**Figure 1H**). Unfortunately, ZL22 was diagnosed with radiation pneumonitis at 11 weeks of transplantation and euthanized at 13 weeks after the

transplantation, at which point γ-globin level was 7.5%. Transient γ-globin induction has been reported for conditions resulting in stress erythropoiesis such as recovery from anemia due to transient erythroblastopenia of childhood (23), BM transplantation (24), and phlebotomy (25, 26). Autologous hematopoietic transplantation of rhesus macaques produces transient expression of γ-globin up to a maximum of 0.99-2.53% at 4-9 weeks of transplantation that stabilizes at pre-transplantation levels after 20 weeks post-transplantation (27), suggesting that most of the γ-globin induction observed in ZL22 and ZL25 was due to *BCL11A* editing.

Stable engraftment with biallelic edited HSCs after low-dose autologous HSPC infusion

To further investigate γ-globin induction potential of *BCL11A* editing in rhesus monkeys, we transplanted two monkeys with HSPCs edited solely at the *BCL11A* enhancer (n = 2, ZM26 and ZM17) as cohort 2. We used 3×NLS-SpCas9, which in previous human HSPC studies was associated with highly efficient indel generation in engrafting HSCs (12). Furthermore, we cryopreserved HSPCs prior to infusion to more fully mimic an anticipated clinical protocol. Consistent with cohort 1 animals, these animals engrafted with typical kinetics, and rescued cell counts and Hb levels at 2-3 weeks post-transplantation similar to control transplanted animals (**Supplemental Figure 4**). Despite having high indel rates (84.9%) in the infusion product of ZM26, and robust ex vivo γ-globin induction (65.9% vs 24.7% in non-edited control), there was a significant drop in the indel frequencies (~25-30%) at 4 weeks post-transplantation that stabilized to ~5-16% at 28 weeks post-transplantation (**Figure 2A, Supplemental Figure 6A-C**). For prior efficient autologous reconstitution by gene marked HSCs after lentiviral gene transfer, we have infused cell products of at least ~3x10^6 CD34+ HSPCs/kg (28, 29). The relatively low infused HSPC number of 1.78×10^6 CD34+ HSPCs/kg could have contributed to inefficient autologous engraftment of the edited cells (**Table 1**). We observed that the *BCL11A* enhancer indels were mainly distributed in biallelic edited BM MNC-derived colonies (~80%) as compared to monoallelic edited colonies (~20%) (**Figure 2B**). γ-globin expression in ZM26

peaked at 8.1% at 6 weeks post-transplantation but decreased to levels indistinguishable from control animals (~0.5%) 20 weeks after transplantation (**Figure 2C**). The clonogenic capacity of BM MNCs of ZM26 at 38 weeks post-transplant was similar to other edited and non-edited animals (**Supplemental Figure 5E-I**).

Erythropoiesis stress induces substantial γ-globin levels in edited animals

As γ-globin induction peaked in the first 12 weeks following transplantation, we hypothesized that stress erythropoiesis might be reinforcing *BCL11A* editing-related γ-globin induction. To test this idea, we phlebotomized edited animals (ZL25 and ZM26) along with non-transplanted (ZL12 and ZM19) and lentivirally transduced (GFP vector) CD34+ HSPC transplanted (RQ7278 and RQ7674) control animals twice a week (20% of total blood volume) for 6 weeks. Following phlebotomy, we observed anemia and elevated reticulocyte counts, with peak reticulocytosis 2-5 weeks after onset of phlebotomy (**Figure 2D, 2E**), consistent with accelerated erythropoiesis kinetics. ZM26, the animal with ~6% indel frequency with indels mainly distributed within biallelic edited colonies (**Figure 2B**) demonstrated substantial γ-globin induction (from 0.6% to 4.4% after 6 weeks of phlebotomy) (**Figure 2F**). In contrast ZL25, the animal with ~3% indel frequency, with indels mainly distributed within monoallelically edited colonies (**Figure 1G**) showed more modest γ-globin induction (from 0.4% to 1% after 6 weeks of phlebotomy). Control non-transplanted and marker vector transduced transplanted animals showed minimal γ-globin induction (from ~0.2-0.3% to ~0.5-0.7% after 6 weeks of phlebotomy), Editing frequencies in ZL25 and ZM26 for both *AAVS1* and *BCL11A* enhancer did not change during the phlebotomy experiment (**Supplemental Figure 6D-F**), indicating that stress erythropoiesis did not preferentially drive hematopoiesis from edited compared to non-edited cells. After terminating phlebotomy, γ-globin expression returned to pre-phlebotomy levels for all animals, along with stable indel frequencies (**Figure 2F**). Together, the phlebotomy and

autologous reconstitution results suggest a positive interactive effect between biallelic *BCL11A* enhancer editing and stress erythropoiesis with regard to γ-globin induction.

Efficient engraftment of BCL11A edited HSPCs

The indel frequency in the input cell product for ZM17, the second animal in cohort 2, was 80.9%. A higher HSPC dose of 6.06×10^6 CD34+ HSPCs/kg was infused to ZM17 (3.4-fold greater than infused to ZM26). Stable indel frequencies were detected in both PB granulocyte (75.1%) and lymphocyte (79.0%) fractions at 25 weeks post-transplantation (**Figure 3A, Supplemental Figure 7A**). Unfortunately, the animal ZM17 developed severe radiation pneumonitis and was euthanized at 28 weeks. 83.6% of edited BM MNC colonies had biallelic indels, 9.8% had monoallelic indels, and 6.6% were unedited (**Figure 3B)**. γ-globin expression in PB reached up to 28.6% at 7 weeks post-transplantation (**Figure 3C**). Like the other animals, γ-globin in ZM17 decreased after autologous transplant, nadiring at 9.9% at 25 weeks and then 12.7% at 28 weeks post-transplantation. Comparing all four edited animals, there was a strong correlation between *BCL11A* enhancer indel frequencies and peak γ-globin levels in peripheral blood during the first 13 weeks following transplantation ($R^2 = 0.73$, $P < 0.001$, **Figure 3D**).

BCL11A plays critical roles in B-lymphocyte maturation and HSC self-renewal (30-32). The rationale of editing the *BCL11A* erythroid enhancer is to minimize impact on non-erythroid hematopoietic functions. To test any selective impact of *BCL11A* enhancer editing on various hematopoietic lineages, different cell fractions from both PB and BM MNCs of ZM17 at 28 weeks post-transplantation were sorted and subjected to deep sequencing. The *BCL11A* enhancer indel frequencies ranged from 78-81% across all PB and BM lineages (excluding CD3+ T-cells with 63% indels), including CD20+ B-lymphoid, CD14+ myeloid cells, CD34+ HSPCs, and CD71+ CD45- erythroblasts, suggesting no selective toxicity to any cell lineage tested (**Figure 3E**, **3F**).

We further analyzed the subset of specific gene edit alleles for which the frequency was at least 1% in one lineage, comprising 14 indels plus the unedited allele. Overall, the distribution of gene edits showed a very similar pattern among all hematopoietic lineages, suggesting the absence of strong lineage-specific selection pressure **(Supplemental Figure 8A)**. In order to measure the similarity among cell subpopulations, we performed an unsupervised hierarchical clustering analysis (using Ward distance) on normalized (z-scored) edit frequencies **(Figure 3G)**. The lineages were grouped in 3 main clusters: 1) CD3+ T-cells in BM and PB; 2) all other PB lineages plus BM CD20+ B-cells; and 3) all other BM lineages. Multiple factors might contribute to this clustering configuration, such as the hierarchical nature of hematopoietic differentiation and heterogeneity in lifespan of lineage-biased HSPCs. We also tested the correlation (Pearson's coefficient) among all possible pairs of lineages using the edit frequency data (**Supplemental Figure 8B, Supplemental Tables 1-2)**. BM and PB CD3+ T-cells showed a significant positive correlation with each other and negative association with PB CD14+ monocytes and PB granulocytes. Positive association was also measured among: BM CD14+ monocytes and BM granulocytes; BM monocytes and CD71+ CD45- erythroblasts; and all PB lineages (besides CD3+ T cells).

Peripheral blood counts, including Hb level and reticulocyte counts of ZM17 at 6 months post-transplantation were not different from those of untransplanted controls (ZL12 and ZM19) and GFP expressing lentivirus transduced CD34+ HSPC transplanted animals (RQ7278 and RQ7674) (**Figure 3H, Supplemental Figure 4**). Furthermore, similar clonogenicity of BM MNCs collected at 28 weeks post-transplantation was observed as compared to other edited animals and the control non-transplanted animal (**Supplemental Figure 5E-I**). Together, these data do not indicate apparent hematologic or erythroid effects of *BCL11A* enhancer editing aside from γ-globin induction.

The most common alleles in rhesus HSPCs after *BCL11A* enhancer editing were a 1-base pair (bp) T insertion, produced by non-homologous end joining (NHEJ) repair, followed by

a -15 bp deletion, produced by MMEJ repair (**Supplemental Figure 9-10**). These predominant edits were the same as observed in human HSPCs after *BCL11A* enhancer editing with the identical sgRNA (12). Previously we observed that engrafting human hematopoietic cells in mouse xenografts preferentially carried NHEJ repair alleles as compared to MMEJ repair alleles. To evaluate the engraftment potential of HSPCs repaired by NHEJ as compared to MMEJ, we analyzed individual gene edit alleles in input HSPCs and engrafting granulocytes and lymphocytes (**Supplemental Figure 9A-F**). We observed that overall edits were variably reduced in the 4 animals comparing the input cell products to engrafting cells (**Supplemental Figure 9, 11**). In each animal, we observed that the fraction of MMEJ alleles at the *BCL11A* enhancer was selectively reduced (1.6 - 4.5-fold) in engrafted cells as compared to the input cell product (**Figure 4A, Supplemental Figure 11**). Similar selective reduction of MMEJ repair alleles in engrafting cells (3.4 - 3.9-fold) was also observed after *AAVS1* editing (**Figure 4B, Supplemental Figure 9A, 9C, 11**).

We calculated the population diversity of gene edit alleles (excluding the unedited allele) as measured by the Shannon H index (33) in each input cell product and engrafted granulocyte and lymphocyte sample. We found that for each animal and sgRNA, there was a consistent reduction in the diversity in the engrafted cells with respect to the input cell product (**Figure 4C, 4D, Supplemental Table 3**). For ZM17, after the initial drop, the diversity of the edited cell population stabilized around H = 2.6, similar for both granulocytes and lymphocytes. This suggests a polyclonal distribution in which: 1) a considerable number of cells bearing different edits engrafted (~250 alleles); 2) the number of alleles with a significant abundance was high; 3) the composition of this population was constant over time; and 4) any in vivo selection acts similarly in the two lineages. For all other animals, the clonality index decreased over time, approaching H < 1, suggesting that the edited cell populations lost more substantial complexity and heterogeneity, tending to an oligoclonal distribution, relative to ZM17. The number of detected edits in the engrafted population reduced over time to ~10-40 alleles, with few alleles

having high relative abundance. In lymphocytes, Shannon's H index decreased more slowly as compared to granulocytes, perhaps due to differences in the lifespan of lineage-biased progenitors in the input product or to a slower turnover of lymphocytes. For animals ZL22 and ZL25, the *AAVS1* and *BCL11A* enhancer edits showed similar clonality dynamics. The H-index at week 12 was positively correlated to infused cell number, consistent with observations from human hematopoietic gene therapy that infused cell number is a key determinant of polyclonal engraftment of gene marked cells ($R^2 = 0.86$, **Figure 4D**) (34).

We performed CIRCLE-seq (35) to empirically define rhesus genomic sites susceptible to off-target in vitro RNP cleavage. Then we performed amplicon deep sequencing of the top 26 candidate off-target sites (based on CIRCLE-seq read counts) in each of the 4 input *BCL11A* enhancer edited input cell products as well as in engrafted hematopoietic cells. Despite detecting robust on-target *BCL11A* enhancer editing in each sample, we did not observe off-target gene editing at any of these 26 sites in any of the samples, at a limit of detection of 0.1% allele frequency (**Figure 4E**).

Discussion

Developing innovative autologous hematopoietic cell transplantation protocols in rhesus macaques is especially complex in that the procedures and reagents for HSC mobilization, collection, gene modification, culture, and re-engraftment are largely adapted from protocols initially optimized for human cells. One challenge we encountered was to achieve consistently safe and effective myeloablation (36, 37), with two animals succumbing to radiation pneumonitis. Furthermore, we obtained variable recovery from mobilized peripheral blood cell apheresis. Three of the four infusion cell products included fewer than the typical target of $3x10^6$ CD34+ HSPCs/kg (**Table 1**), which might disadvantage the engraftment of the cell product as compared to residual HSCs. Despite these challenges, by investigating just 4 animals, we observed improved gene-editing efficiency from ~30-40% to ~80-85% indels in the input cell product at scale to support autologous hematopoietic transplantation following myeloablative conditioning therapy. We demonstrated a proof-of-principle for therapeutic gene editing with ~70-80% gene modifications in engrafting hematopoietic cells after 28 weeks, mainly distributed as biallelic edits. This result is the most efficient autologous hematopoietic gene editing achieved in non-human primates to our knowledge. Prior reports demonstrated substantially fewer gene edits in engrafting hematopoietic cells (14, 21). In a previous NHP setting, editing of the *CCR5* gene dropped from 40% in the infusion product to 3-5% at 6 months (22). A recent study aiming to induce HbF by creating hereditary persistence of fetal hemoglobin (HPFH) mutation in rhesus macaques showed a decrease in indels from ~70% in the input cell product to ~15% in engrafting cells (21). These results suggest that at intermediate editing frequencies, indels in unfractionated autologous HSPCs also may overestimate those in engrafting HSCs (12). A non-mutually exclusive possibility could be incomplete hematopoietic ablation with partial reconstitution by residual non-ablated HSCs. These results encourage the development of gene editing protocols to maximize both the total number and fraction of biallelically modified HSCs.

We observed selective reduction of MMEJ repair alleles in engrafting compared to input cells. This result suggests that HSCs, a rare subset within HSPC cell products, preferentially repair by NHEJ. NHEJ repair with short indels appears sufficient to disrupt *BCL11A* enhancer function and support HbF induction in erythroid progeny of edited HSCs. We found that *BCL11A* enhancer editing yielded robust induction of γ-globin during steady-state erythropoiesis, with ~18-fold increase from unedited steady-state level in the same animal (**Figure 3C, Supplemental Figure 7B**). In addition, we observed a substantial positive interaction between *BCL11A* enhancer editing and stress erythropoiesis associated with hematopoietic repopulation, with an additional 2.8 - 6.8-fold increase as compared to the steady-state levels in the edited animals. During phlebotomy induced erythroid stress, we observed HbF induction only in ZM26, the animal with *BCL11A* enhancer edits mainly distributed as biallelic indels, also consistent with a positive interaction between erythroid stress and BCL11A modulation. Future studies appear warranted to further explore this interaction. In the setting of HbF induction for β-hemoglobinopathy patients as compared to healthy individuals, we anticipate there may be additional contributions from both disease-associated stress erythropoiesis as well as survival advantage of HbF expressing erythrocytes and precursors. Together, we predict these effects, plus more pancellular than heterocellular distributions of gene edits, could further magnify the impact of HbF induction following *BCL11A* enhancer editing in β-hemoglobinopathy patients.

For all animals and guide RNAs (including targeting both *AAVS1* and *BCL11A* enhancer), we observed a reduction of the diversity of gene edits in the engrafted cells with respect to the input cell product. The starting cell product was relatively complex, with edits more evenly distributed. The engrafted cells had fewer edits, suggesting a bottleneck in the initial engrafting cell population, that then stabilized over extended examination. Cell products with greater HSPC numbers were associated with more polyclonal engraftment. These dynamics appear reminiscent of gene therapy with HSCs marked by lentiviral insertions.

Under efficient editing conditions, we observed a similar distribution of *BCL11A* enhancer indels across all PB and BM lineages (with exception of modestly lower frequency of gene editing in long-lived CD3+ T-lymphocytes) suggesting no skewed hematopoietic contributions of *BCL11A* enhancer gene-edited cells. Moreover, we observed normal blood counts including no anemia or hemolysis following efficient *BCL11A* enhancer editing, consistent with intact hematopoiesis and erythropoiesis. Off-target genotoxicity is one possible concern of therapeutic gene editing. We did not observe any off-target gene edits attributable to *BCL11A* enhancer editing, although large deletions and rearrangements were not specifically evaluated (38). These findings are similar to the absence of apparent toxicity of *BCL11A* enhancer editing with 3×NLS-SpCas9 and sgRNA-#1617 in human HSPCs (12).

In summary, we evaluated the clinical potential of autologous *BCL11A* erythroid enhancer editing in rhesus macaques. *BCL11A* enhancer edited HSCs can persist for at least 101 weeks post-transplant and provide potentially therapeutic levels of HbF in PB RBCs without anemia or other apparent hematologic toxicity. These results emphasize that gene editing efficiency and repair mode, input CD34+ HSPC number and conditioning therapy are each critical variables that influence gene edits in engrafted hematopoietic cells following autologous HSCT. Overall, these findings support *BCL11A* erythroid enhancer genome editing as a promising strategy for HbF induction for β-hemoglobinopathies.

Methods

Detailed methods are provided in the Supplemental Methods. All raw sequence data have been deposited at NCBI Sequence Read Archive (SRA) under the accession number of PRJNA655555.

Study approval

Rhesus macaques (*Macaca mulatta*) were housed and handled in accordance with the guidelines set by the Committee on Care and Use of Laboratory Animals of the Institute of Laboratory Animal Resources, National Research Council, and all animal protocols were approved by the Animal Care and Use Committee of the National Heart, Lung, and Blood Institute-NHLBI (approved protocol no: H-0136R4).

Statistics

Standard errors of the mean are given as error bars in all figures. The data were statistically analyzed with one-way analysis of variance (ANOVA) followed by the Tukey post hoc test using GraphPad Prism 7 software (GraphPad Software, Inc, USA). Data were considered significantly different at $p < 0.05$. Clonality index and lineage data analysis were performed by means of R statistical software (39) and packages vegan and ggplots.

Author contributions

SD and JZ design, performed, and analyzed experiments, prepared figures, and wrote the manuscript. AHS helped with figures and analysis. DP , SNP, and SMP-M performed the clonality analyses. YW, NU, JG, MY, CD, JB, JJH, AL, and TN helped with experiments. ACB, AEK, NSL, TE, and RED performed animal care, transplantation, and sample derivation. KL and SAW produced 3×NLS SpCas9 protein. CRL, SQT, and MW performed and analyzed off-target assays. DEB and JFT designed and analyzed experiments and wrote the manuscript.

Acknowledgments

The authors thank the NIH/NHLBI Biochemistry core facility for the HPLC service. D.E.B. was supported by NHLBI (P01HL053749), St. Jude Children's Research Hospital Collaborative Research Consortium, and Burroughs Wellcome Fund. K.L. and S.A.W. were supported in part by NIH grants F31HL147482 and R01GM115911.

References

1. Tisdale J. Improvements in haploidentical transplantation for sickle cell disease and β-thalassaemia. *Lancet Haematol.* 2019;6(4):e168-e169.
2. Eaton WA, and Bunn HF. Treating sickle cell disease by targeting HbS polymerization. *Blood.* 2017;129(20):2719-2726.
3. Thein SL. The emerging role of fetal hemoglobin induction in non-transfusion-dependent thalassemia. *Blood Rev.* 2012;26:S35-S39.
4. Menzel S, Garner C, Gut I, Matsuda F, Yamaguchi M, Heath S, et al. A QTL influencing F cell production maps to a gene encoding a zinc-finger protein on chromosome 2p15. *Nat Genet.* 2007;39(10):1197-1199.
5. Uda M, Galanello R, Sanna S, Lettre G, Sankaran VG, Chen W, et al. Genome-wide association study shows BCL11A associated with persistent fetal hemoglobin and amelioration of the phenotype of β-thalassemia. *Proc Natl Acad Sci.* 2008;105(5):1620-1625.
6. Sankaran VG, Menne TF, Xu J, Akie TE, Lettre G, Van Handel B, et al. Human fetal hemoglobin expression is regulated by the developmental stage-specific repressor BCL11A. *Science.* 2008;322(5909):1839-1842.
7. Sankaran VG, Xu J, Ragoczy T, Ippolito GC, Walkley CR, Maika SD, et al. Developmental and species-divergent globin switching are driven by BCL11A. *Nature.* 2009;460(7259):1093-1097.
8. Bauer DE, Kamran SC, Lessard S, Xu J, Fujiwara Y, Lin C, et al. An erythroid enhancer of BCL11A subject to genetic variation determines fetal hemoglobin level. *Science.* 2013;342(6155):253-257.
9. Canver MC, Smith EC, Sher F, Pinello L, Sanjana NE, Shalem O, et al. BCL11A enhancer dissection by Cas9-mediated in situ saturating mutagenesis. *Nature.* 2015;527(7577):192-197.

10. Smith EC, Luc S, Croney DM, Woodworth MB, Greig LC, Fujiwara Y, et al. Strict in vivo specificity of the Bcl11a erythroid enhancer. *Blood.* 2016;128(19):2338-2342.
11. Vierstra J, Reik A, Chang K-H, Stehling-Sun S, Zhou Y, Hinkley SJ, et al. Functional footprinting of regulatory DNA. *Nat Methods.* 2015;12(10):927-930.
12. Wu Y, Zeng J, Roscoe BP, Liu P, Yao Q, Lazzarotto CR, et al. Highly efficient therapeutic gene editing of human hematopoietic stem cells. *Nat Med.* 2019;25(5):776-783.
13. Kiem H-P, Arumugam PI, Burtner CR, Fox CF, Beard BC, Dexheimer P, et al. Pigtailed macaques as a model to study long-term safety of lentivirus vector-mediated gene therapy for hemoglobinopathies. *Mol Ther Methods Clin Dev.* 2014;1:14055.
14. Kim MY, Yu K-R, Kenderian SS, Ruella M, Chen S, Shin T-H, et al. Genetic inactivation of CD33 in hematopoietic stem cells to enable CAR T cell immunotherapy for acute myeloid leukemia. *Cell.* 2018;173(6):1439-1453. e1419.
15. Uchida N, Hsieh MM, Raines L, Haro-Mora JJ, Demirci S, Bonifacino AC, et al. Development of a forward-oriented therapeutic lentiviral vector for hemoglobin disorders. *Nat Commun.* 2019;10(1):1-14.
16. Johnson RM, Buck S, Chiu CH, Gage DA, Shen TL, Hendrickx AG, et al. Humans and old world monkeys have similar patterns of fetal globin expression. *J Exp Zool.* 2000;288(4):318-326.
17. Donahue RE, and Dunbar CE. Update on the use of nonhuman primate models for preclinical testing of gene therapy approaches targeting hematopoietic cells. *Hum Gene Ther.* 2001;12(6):607-617.
18. Koelle SJ, Espinoza DA, Wu C, Xu J, Lu R, Li B, et al. Quantitative stability of hematopoietic stem and progenitor cell clonal output in rhesus macaques receiving transplants. *Blood.* 2017;129(11):1448-1457.

19. Shepherd BE, Kiem H-P, Lansdorp PM, Dunbar CE, Aubert G, LaRochelle A, et al. Hematopoietic stem-cell behavior in nonhuman primates. *Blood.* 2007;110(6):1806-1813.

20. Bae S, Kweon J, Kim HS, and Kim J-S. Microhomology-based choice of Cas9 nuclease target sites. *Nat Methods.* 2014;11(7):705-706.

21. Humbert O, Radtke S, Samuelson C, Carrillo RR, Perez AM, Reddy SS, et al. Therapeutically relevant engraftment of a CRISPR-Cas9–edited HSC-enriched population with HbF reactivation in nonhuman primates. *Sci Transl Med.* 2019;11(503):eaaw3768.

22. Peterson CW, Wang J, Norman KK, Norgaard ZK, Humbert O, Collette KT, et al. Long-term multilineage engraftment of autologous genome-edited hematopoietic stem cells in nonhuman primates. *Blood.* 2016;127(20):2416-2426.

23. Papayannopoulou T, Vichinsky E, and Stamatoyannopoulos G. Fetal Hb Production during Acute Erythroid Expansion: I. OBSERVATIONS IN PATIENTS WITH TRANSIENT ERYTHROBLASTOPENIA AND POST-PHLEBOTOMY. *Br J Haematol.* 1980;44(4):535-546.

24. Ferster A, Corazza F, Vertongen F, Bujan W, Devalck C, Fondu P, et al. Transplanted sickle-cell disease patients with autologous bone marrow recovery after graft failure develop increased levels of fetal haemoglobin which corrects disease severity. *Br J Haematol.* 1995;90(4):804-808.

25. DeSimone J, Biel S, and Heller P. Stimulation of fetal hemoglobin synthesis in baboons by hemolysis and hypoxia. *Proc Natl Acad Sci.* 1978;75(6):2937-2940.

26. McDonagh K, Dover GJ, Donahue R, Nathan D, Byrne E, and Nienhuis A. Hydroxyurea-induced HbF production in anemic primates: augmentation by erythropoietin, hematopoietic growth factors, and sodium butyrate. *Exp Hematol.* 1992;20(10):1156-1164.

27. Demirci S, Mora JJH, Yapundich M, Drysdale C, Gamer J, Nassehi T, et al. Fetal hemoglobin (HbF) and F-cell variance in mobilized CD34+ cell transplanted rhesus monkeys. *Exp Hematol.* 2019;75:21-25.e21.

28. Evans ME, Kumkhaek C, Hsieh MM, Donahue RE, Tisdale JF, and Uchida N. TRIM5α Variations Influence Transduction Efficiency With Lentiviral Vectors in Both Human and Rhesus CD34+ Cells In Vitro and In Vivo. *Mol Ther.* 2014;22(2):348-358.

29. Uchida N, Nassehi T, Drysdale CM, Gamer J, Yapundich M, Bonifacino AC, et al. Busulfan combined with immunosuppression allows efficient engraftment of gene-modified cells in a rhesus macaque model. *Mol Ther.* 2019;27(9):1586-1596.

30. Liu P, Keller JR, Ortiz M, Tessarollo L, Rachel RA, Nakamura T, et al. Bcl11a is essential for normal lymphoid development. *Nat Immunol.* 2003;4(6):525-532.

31. Luc S, Huang J, McEldoon JL, Somuncular E, Li D, Rhodes C, et al. Bcl11a deficiency leads to hematopoietic stem cell defects with an aging-like phenotype. *Cell Rep.* 2016;16(12):3181-3194.

32. Brendel C, Guda S, Renella R, Bauer DE, Canver MC, Kim Y-J, et al. Lineage-specific BCL11A knockdown circumvents toxicities and reverses sickle phenotype. *J Clin Invest.* 2016;126(10):3868-3878.

33. Shannon CE. A mathematical theory of communication. *Bell Syst Tech J.* 1948;27(3):379-423.

34. Six E, Guilloux A, Denis A, Lecoules A, Magnani A, Vilette R, et al. Clonal tracking in gene therapy patients reveals a diversity of human hematopoietic differentiation programs. *Blood.* 2020;135(15):1219-1231.

35. Tsai SQ, Nguyen NT, Malagon-Lopez J, Topkar VV, Aryee MJ, and Joung JK. CIRCLE-seq: a highly sensitive in vitro screen for genome-wide CRISPR–Cas9 nuclease off-targets. *Nat Methods.* 2017;14(6):607-614.

36. Hayakawa J, Hsieh MM, Uchida N, Phang O, and Tisdale JF. Busulfan Produces Efficient Human Cell Engraftment in NOD/LtSz-Scid IL2RγNull Mice. *Stem Cells.* 2009;27(1):175-182.

37. Hsieh MM, Langemeijer S, Wynter A, Phang OA, Kang EM, and Tisdale JF. Low-dose parenteral busulfan provides an extended window for the infusion of hematopoietic stem cells in murine hosts. *Exp Hematol.* 2007;35(9):1415-1420.

38. Kosicki M, Tomberg K, and Bradley A. Repair of double-strand breaks induced by CRISPR–Cas9 leads to large deletions and complex rearrangements. *Nat Biotechnol.* 2018;36(8):765-771.

39. Team RC. R: A language and environment for statistical computing. R Foundation for Statistical Computing, Vienna, Austria. 2013.

Figures

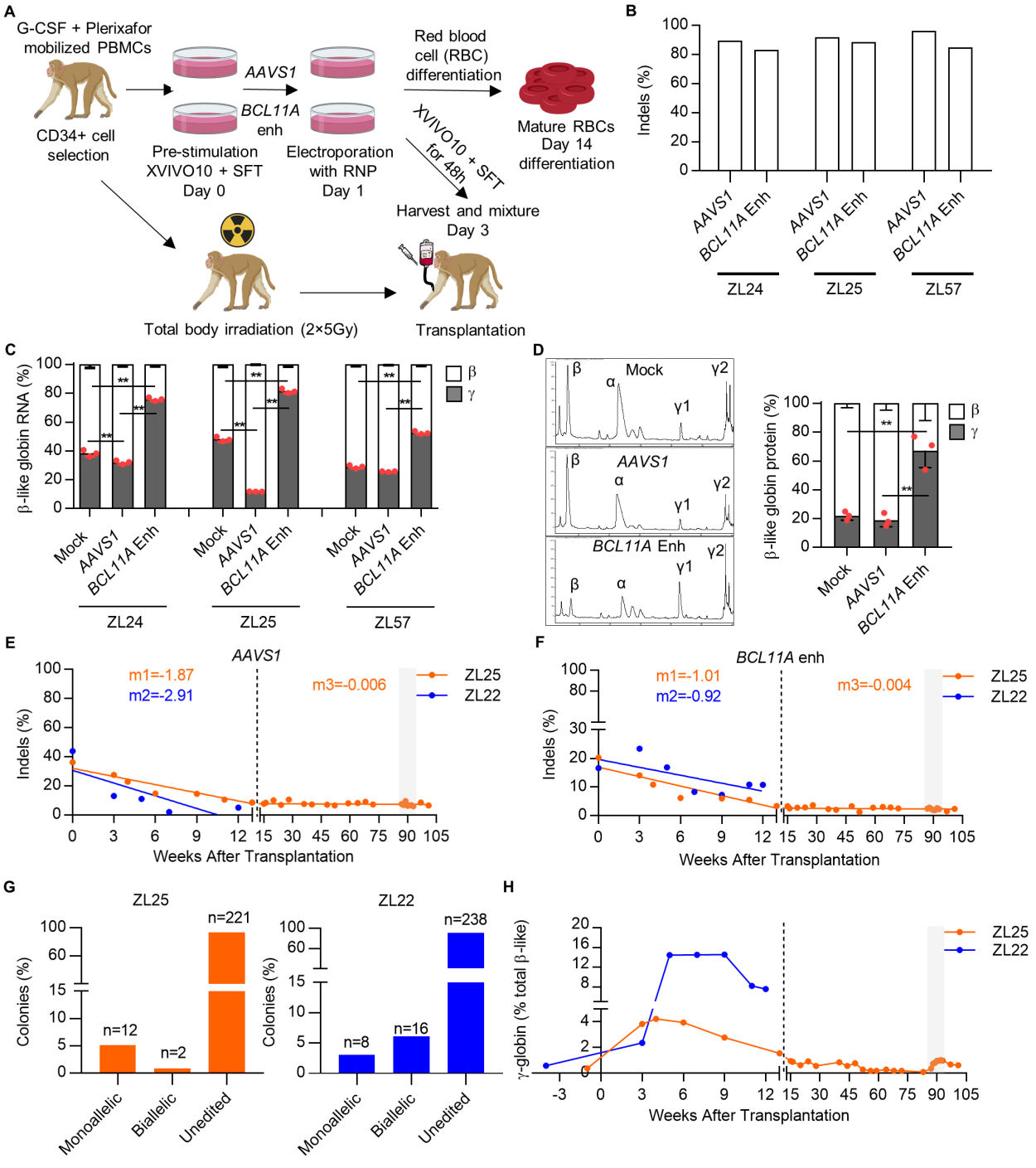

Figure 1. Durable autologous engraftment following *BCL11A* enhancer gene editing. (A) Schematic representation of electroporation of rhesus CD34+ HSPCs with ribonucleoprotein (RNP) complex composed of 2×NLS SpCas9 or 3×NLS SpCas9 protein, and either *BCL11A*

enhancer targeting (#1617) or *AAVS1* targeting sgRNA. The cells are either used for ex vivo analysis or autologous transplantation. (**B**) Editing efficiency measured by Sanger sequencing with TIDE analysis, and (**C**) β-like globin RNA expression by RT-qPCR normalized to α-globin expression in non-edited (Mock), *AAVS1* and *BCL11A* edited rhesus CD34+ HSPCs in small scale (ZL24 and ZL25, 5×10^4 cells, 200 pmol for both SpCas9 and sgRNAs) and large scale (ZL57, 5×10^6 cells, 1000 pmol for both SpCas9 and sgRNAs) electroporation conditions. (n=3, one-way analysis of variance (ANOVA) followed by the Tukey post hoc test, **, $P < 0.01$) (**D**) β-like globin protein expression by reverse phase-high performance liquid chromatography (RP-HPLC), (n=3, one-way analysis of variance (ANOVA) followed by the Tukey post hoc test, ** $P <$ 0.01). ZL25 and ZL22 were transplanted with *AAVS1* and *BCL11A* enhancer edited cells (1:1). The gray rectangle represents the phlebotomy course. Editing frequencies in granulocytes for (**E**) *AAVS1* and (**F**) *BCL11A* enhancer in transplanted rhesus macaques. Slopes were calculated separately for the first 13 weeks of transplantation (early progenitor phase) and later time points (HSC phase) as indicated by the dashed line. (**G**) Distribution of monoallelic and biallelic edited colonies collected from methylcellulose plates for bone marrow mononuclear cells of ZL25 at 100 weeks and ZL22 at 13 weeks post-transplantation. (**H**) γ-globin protein expression percentage in ZL25 and ZL22.

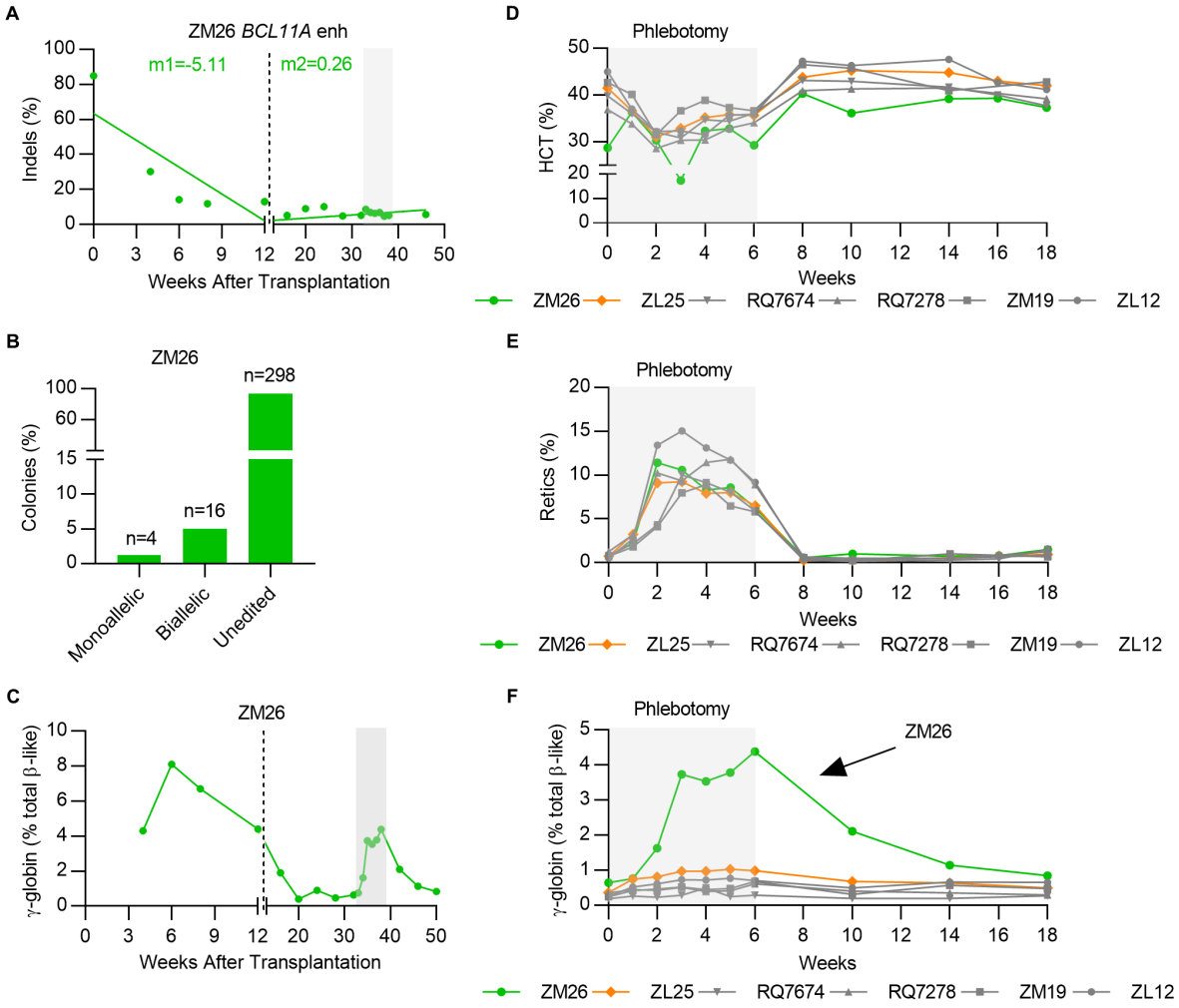

Figure 2. Stress erythropoiesis cooperates with *BCL11A* enhancer editing to amplify γ-globin induction. (A) Editing frequencies in granulocytes of ZM26 transplanted with *BCL11A* edited CD34+ HPSCs. Slopes were calculated separately for the first 13 weeks of transplantation (early progenitor phase) and later time points (HSC phase) as indicated by the dashed line. (**B**) Distribution of monoallelic and biallelic edited colonies collected from methylcellulose plates for bone marrow mononuclear cells of ZM26 at 38 weeks post-transplantation. (**C**) γ-globin protein expression in ZM26. The gray rectangle represents the phlebotomy course. **(D)** Hematocrit (HCT), (**E**) reticulocyte, and (**F**) γ-globin protein percentages in phlebotomized non-transplanted (ZL12 and ZM19), lentivirus (GFP vector) transduced CD34+

HSPC transplanted (RQ7278 and RQ7674), and *BCL11A* enhancer edited animals (ZM26 and ZL25).

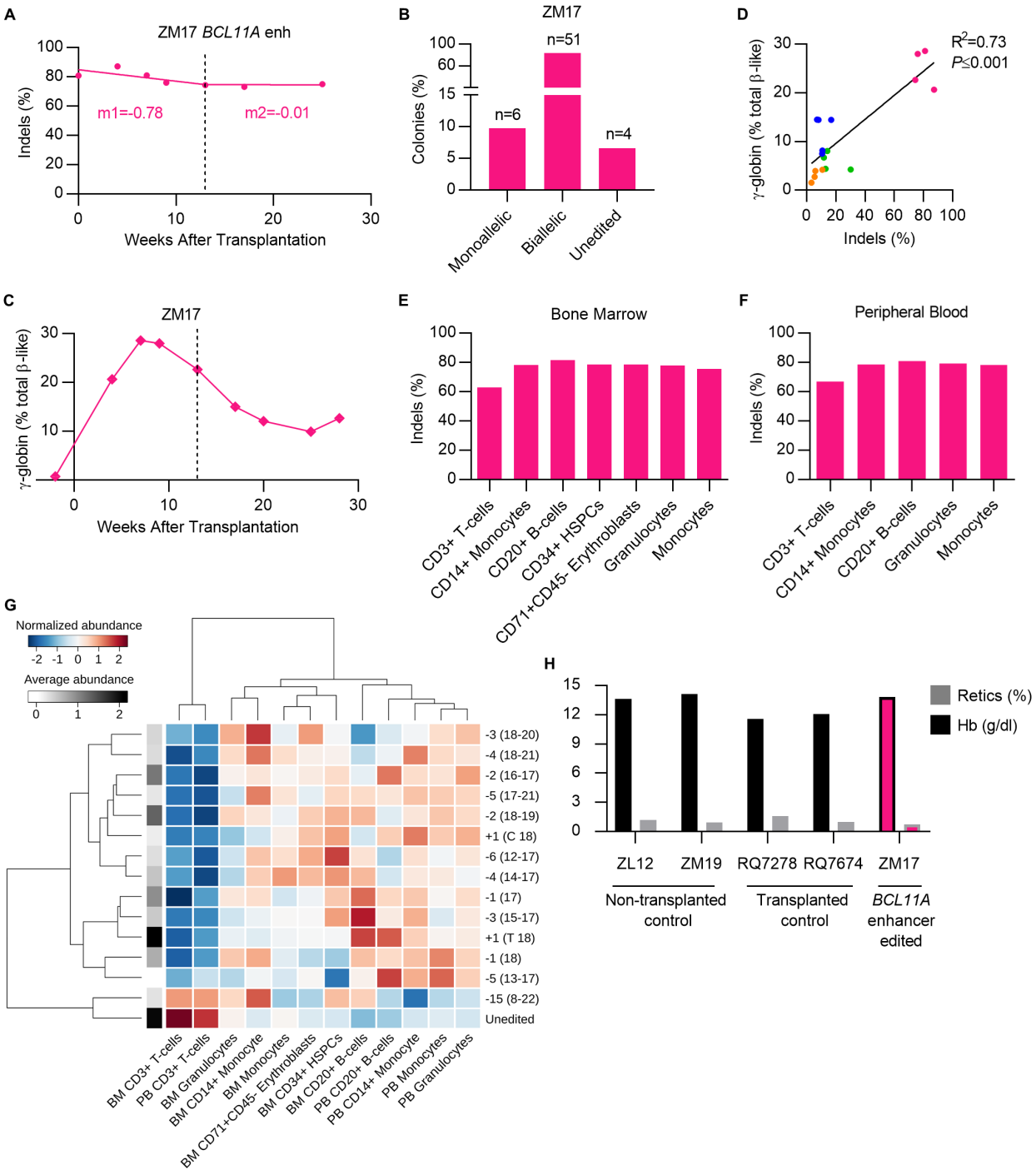

Figure 3. Robust *BCL11A* enhancer editing and γ-globin induction. (**A**) Editing frequencies in granulocyte fraction in ZM17. Slopes were calculated separately for the first 13 weeks of transplantation (early progenitor phase) and later time points (HSC phase) as indicated by the dashed line. (**B**) Distribution of monoallelic and biallelic edited colonies collected from

methylcellulose plates for bone marrow (BM) mononuclear cells of ZM17 at 28 weeks post-transplantation. (**C**) γ-globin protein expression by reverse phase-high performance liquid chromatography (RP-HPLC) in peripheral blood (PB) of ZM17. (**D**) Correlation of editing frequencies in all transplanted animals (4-13 weeks post-transplantation) with γ-globin protein expression by RP-HPLC. (**E**) Editing frequencies in BM-derived CD3+ T-cells, CD14+ monocytes, CD20+ B-cells, CD34+ HSPCs, CD71+ CD45- erythroblasts, and granulocytes and monocytes sorted using FSC A and SSC A. (**F**) Editing frequencies in PB-derived granulocytes, monocytes, CD3+, CD14+, and CD20+ cells. (**G**) Heatmap representation for normalized alleles abundance values among BM and PB lineages of ZM17 at 28 weeks post-transplantation. The allele-specific average abundance value (log) is represented by a gray-scale color on the left side of the heatmap. Both columns (lineages) and rows (alleles) are ordered according to their similarity measured by Ward distance. (**H**) Hemoglobin (Hb) and reticulocyte count percentages in non-transplanted (ZL12 and ZM19), lentivirus (GFP vector) transduced CD34+ HSPC transplanted (RQ7278 and RQ7674), and *BCL11A* enhancer edited animal (ZM17).

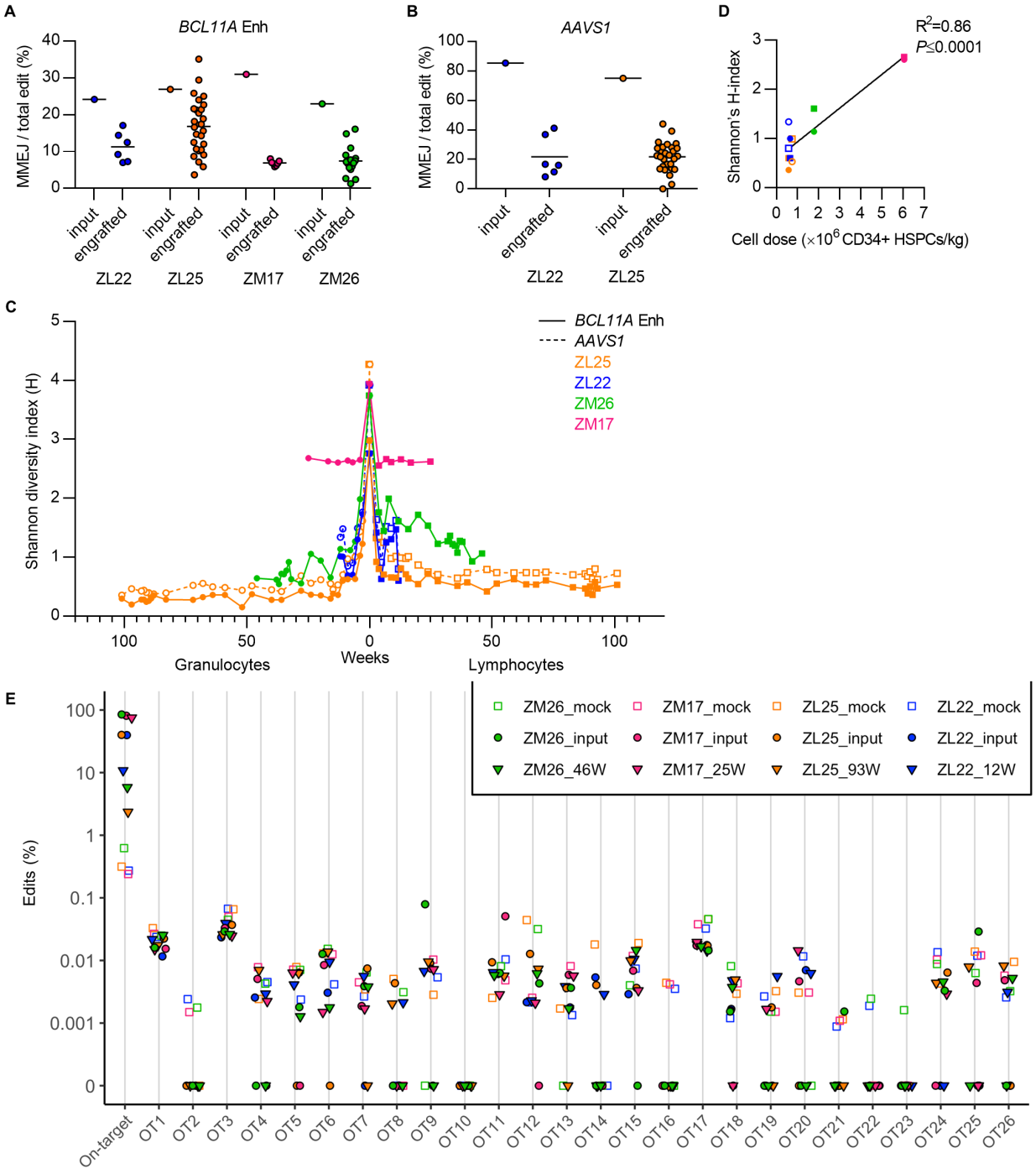

Figure 4. Gene editing dynamics after *BCL11A* enhancer editing. Relative loss of engrafted edits repaired by MMEJ in transplanted animals for (**A**) *BCL11A* enhancer and (**B**) *AAVS1* alleles. Deletions ≥8 bp were categorized as MMEJ, while all other indels were categorized as NHEJ. (**C**) Shannon diversity index (H) for edit distribution in input cell products and engrafted

samples. Granulocytes and lymphoid lineage data are plotted symmetrically, with the former on left (for animal ZL22 and ZL25, both *BCL11A* enhancer and *AAVS1* are reported; for ZM17 and ZM26, only *BCL11A* enhancer data), and (**D**) Correlation of Shannon diversity index (H) with infusion cell dose in all transplanted animals (12-13 weeks post-transplantation). Granulocytes (Circles), Lymphocytes (Squares), *BCL11A* Enhancer (Filled shapes), *AAVS1* (Open shapes). (**E**) Off-target analysis of granulocyte in edited animals transplanted with *BCL11A* enhancer edited CD34+ HSPCs. Using CIRCLE-Seq, 26 potential genomic off-target sites for *BCL11A* enhancer guide #1617 were identified. Editing frequencies at the 26 sites were evaluated through amplicon deep sequencing and analysis. The samples include the infusion product (input) and granulocyte fraction of a later peripheral blood collection for each rhesus macaque. Each point represents a single replicate.

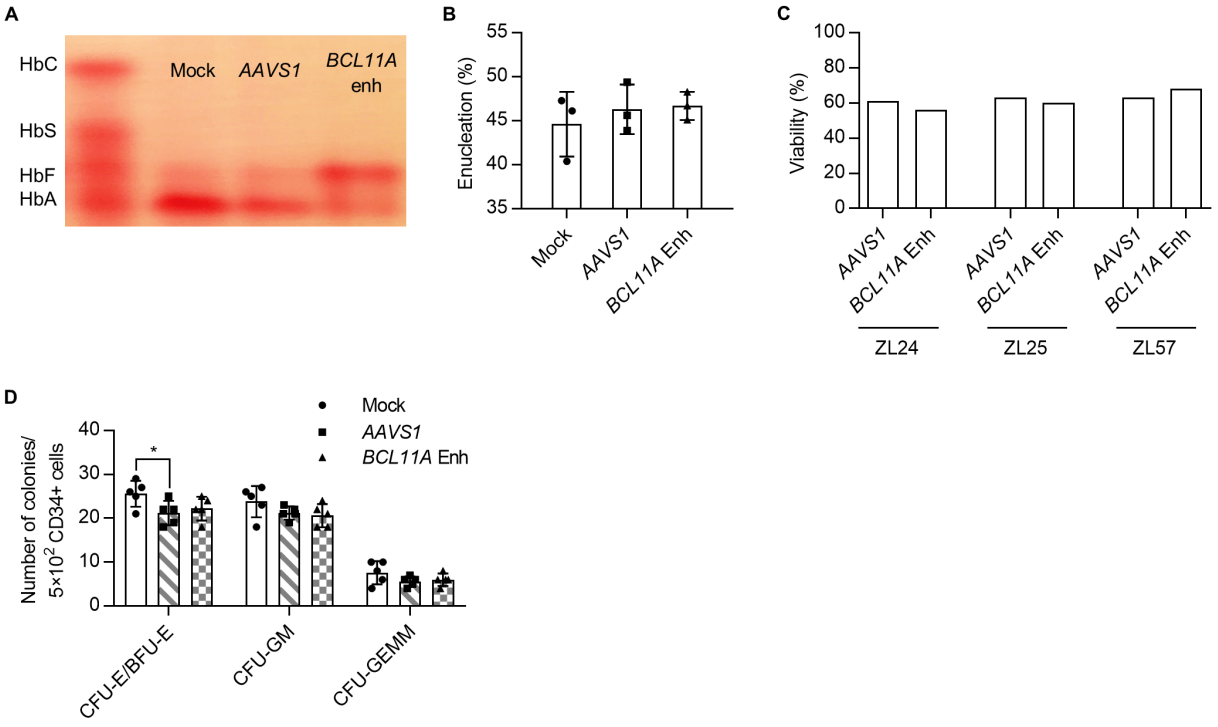

Supplemental Figure 1. *BCL11A* enhancer editing induces γ-globin in rhesus CD34+ HSPCs without affecting colony-forming unit (CFU) formation ability and enucleation. (A) Hemoglobin (Hb) electrophoresis and (**B**) enucleation percentages for ex vivo differentiated red blood cells (RBCs) in non-edited (Mock) and edited (*AAVS1* or *BCL11A* enhancer) rhesus CD34+ HSPCs. (n=3, one-way analysis of variance (ANOVA) followed by the Tukey post hoc test) (**C**) Cell viability of electroporated rhesus CD34+ HSPCs edited for *AAVS1* or *BCL11A* enhancer in small scale (ZL24 and ZL25, 5×10^4 cells, 200pmol for both 2×NLS SpCas9 and sgRNAs) and large scale (ZL57, 1.5×10^6 cells, 1000pmol for both 2×NLS SpCas9 and sgRNAs) electroporation conditions. (**D**) CFU formation ability of CD34+ HSPCs incubated 48 h in ex vivo culture conditions after electroporation with RNP. (n=5, one-way ANOVA followed by the Tukey post hoc test, * $P < 0.05$)

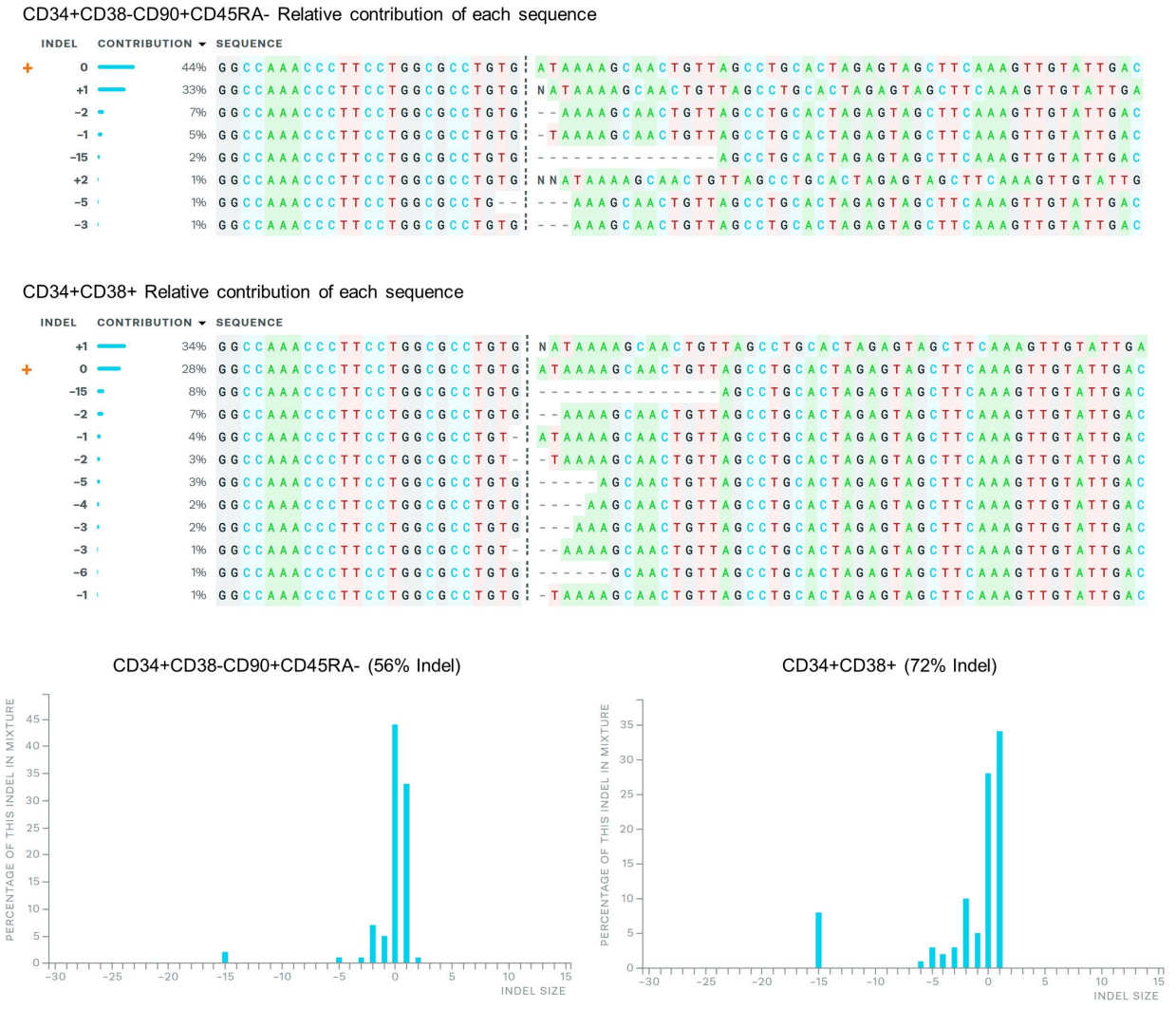

Supplemental Figure 2. Slightly lower indels in the HSC-enriched population with higher indel frequencies repaired by NHEJ compared to committed progenitors. Indel spectrum of rhesus CD34+ HSPCs sorted 2 hours after RNP electroporation for HSC-enriched population (CD34+CD38-CD90+CD45RA-) and committed progenitors (CD34+CD38+). Sanger sequences of the two populations were analyzed using ICE (Synthego).

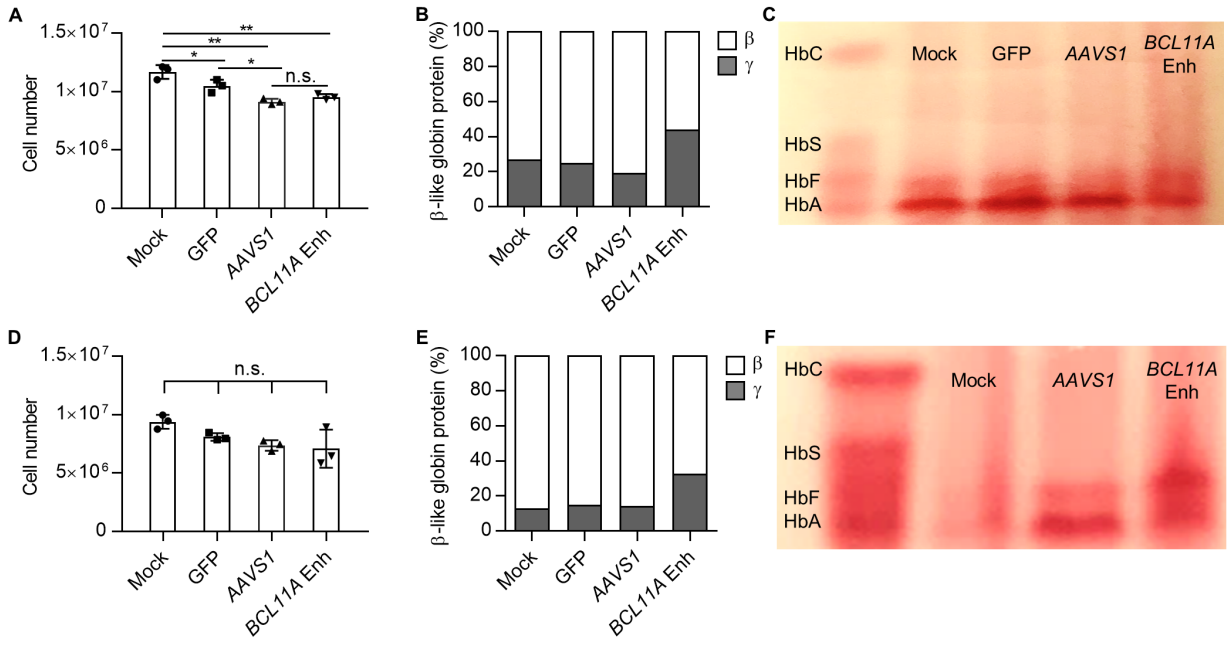

Supplemental Figure 3. Ex vivo γ-globin induction in *BCL11A* enhancer edited rhesus CD34+ HSPCs before transplantation. (A) Cell number (n=3) and β-like globin protein expression by (**B**) reverse phase-high performance liquid chromatography (RP-HPLC) and (**C**) hemoglobin (Hb) electrophoresis in ex vivo differentiated ZL25 CD34+ HSPCs before transplantation. (one-way analysis of variance (ANOVA) followed by the Tukey post hoc test, * $P < 0.05$, ** $P < 0.01$). **(D)** Cell number (n=3) and β-like globin protein expression by (**E**) RP-HPLC and (**F**) Hb electrophoresis in ex vivo differentiated ZL22 CD34+ HSPCs before transplantation.

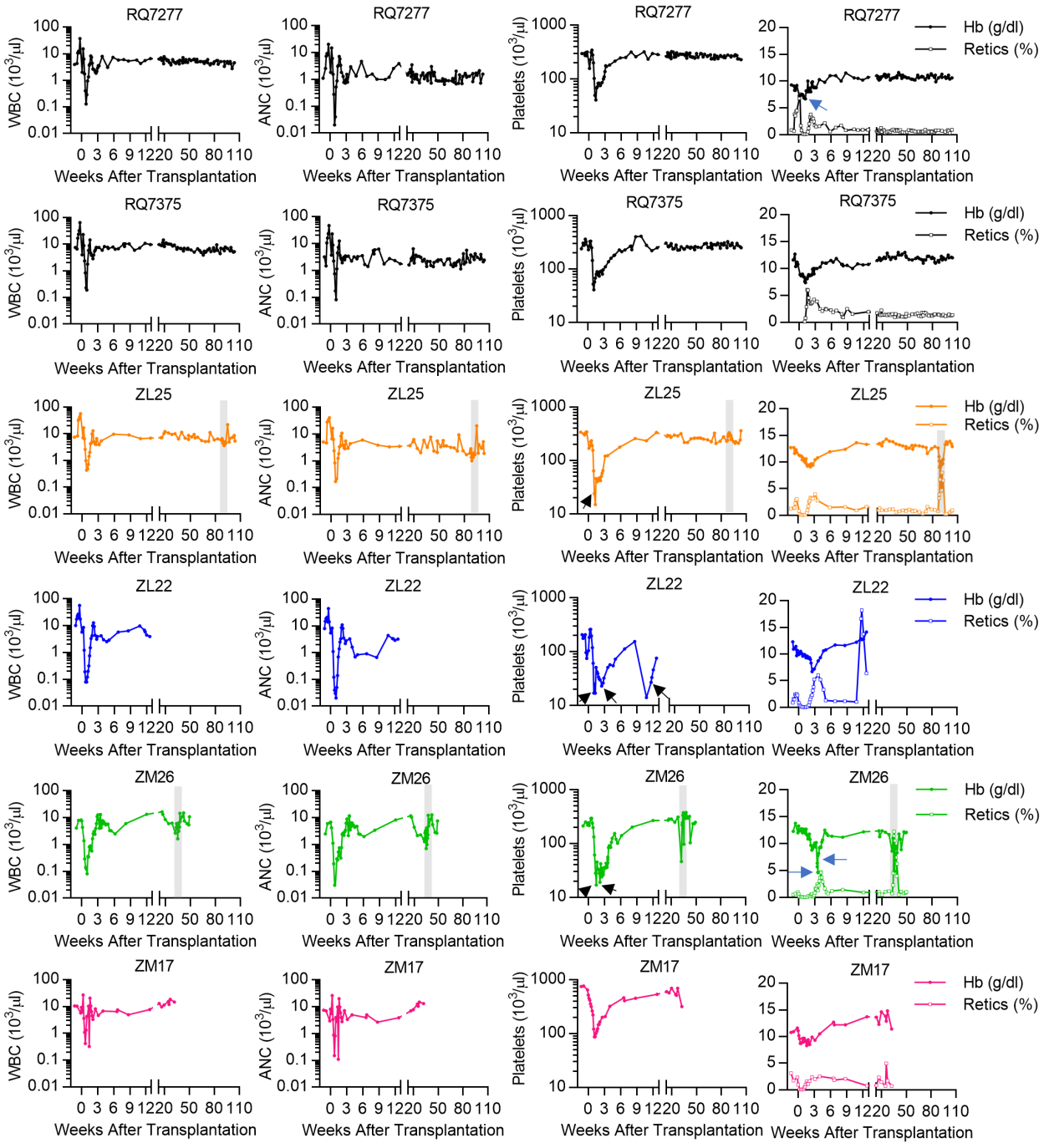

Supplemental Figure 4. Typical autologous reconstitution kinetics following *BCL11A* enhancer gene editing. *BCL11A* enhancer edited CD34+ HSPC transplanted animals (ZL25, ZL22, ZM26, and ZM17) rescued their cell counts and hemoglobin (Hb) levels with typical kinetics similar to control animals transplanted with lentivirus (GFP vector) transduced CD34+

HSPCs (RQ7277 and RQ7375). The black arrow indicates platelet transfusion and the blue arrow indicates whole blood transfusion. The gray rectangle represents the phlebotomy course.

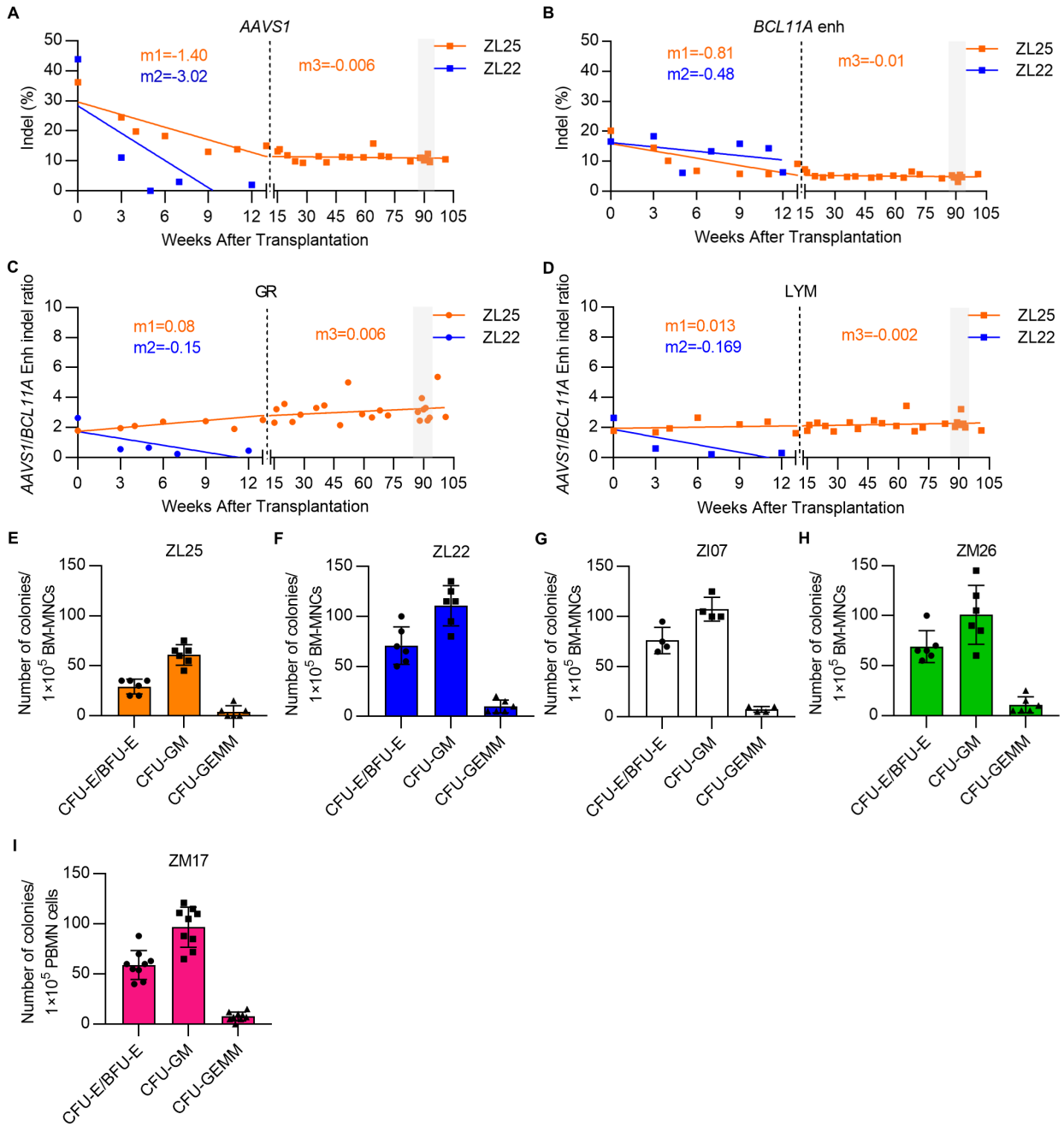

Supplemental Figure 5. **Durable autologous engraftment and colony-forming unit (CFU) potential following *BCL11A* enhancer gene editing.** ZL25 and ZL22 were transplanted with *AAVS1* and *BCL11A* enhancer edited cells (1:1). The gray rectangle represents the phlebotomy course. Editing frequencies in lymphocyte (LYM) fractions for (**A**) *AAVS1* and (**B**) *BCL11A* enhancer in transplanted rhesus macaques. *AAVS1*/1617 editing ratio in (**C**) granulocyte (GR)

and (**D**) LYM fractions of the transplanted animals. CFU potential of BM MNCs of (**E**) ZL25 at 100 weeks post-transplantation (n=6), (**F**) ZL22 at 13 weeks post-transplantation (n=6), (**G**) a non-transplanted control animal, ZI07 (n=4), (**H**) ZM26 at 38 weeks post-transplantation (n=6), and ZM17 at 28 weeks post-transplantation (n=9).

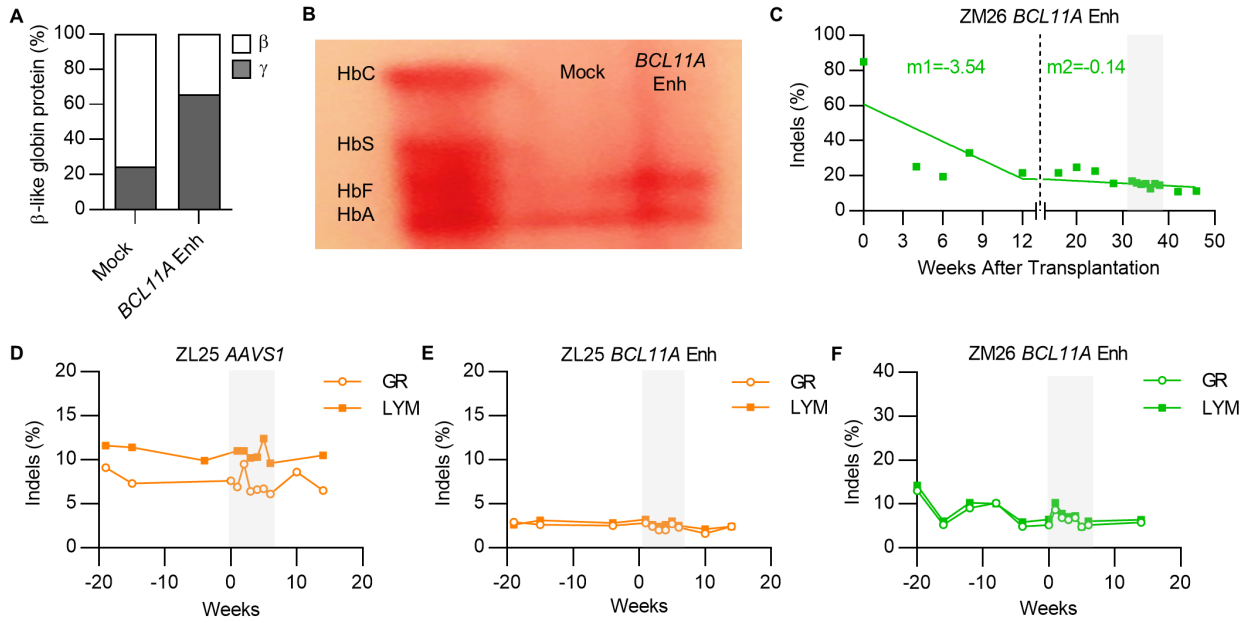

Supplemental Figure 6. **Stable gene editing dynamics after transplantation and during phlebotomy.** (**A**) Reverse-phase high-performance liquid chromatography (RP-HPLC) and (**B**) hemoglobin (Hb) electrophoresis analysis for β-like globin protein expression evaluation in ex vivo differentiated red blood cells (RBCs) of non-edited (Mock) and *BCL11A* enhancer edited rhesus CD34+ HSPCs of ZM26 before transplantation. (**C**) Indel frequencies in the lymphocyte (LYM) fraction of ZM26 over time. Indel percentages during the phlebotomy course for (**D**) *AAVS1* and (**E**) *BCL11A* enhancer in ZL25, and (**F**) *BCL11A* enhancer in ZM26 for granulocytes (GR) and LYM fractions.

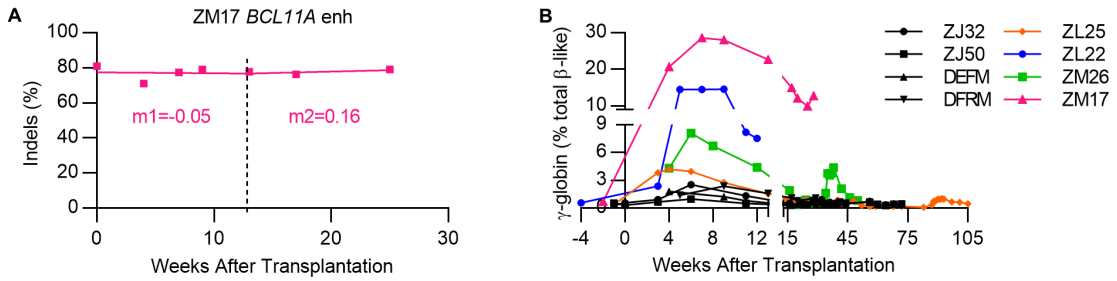

Supplemental Figure 7. Robust *BCL11A* enhancer editing and γ-globin induction. (**A**) Indel frequencies in lymphocyte fraction of ZM17 over time. (**B**) γ-globin protein expression in animals transplanted with lentivirus transduced (GFP/YFP vector) (DEFM, DFRM, ZJ32, and ZJ50) (27), or *BCL11A* enhancer edited (ZL25, ZL22, ZM26, and ZM17) CD34+ HSPCs.

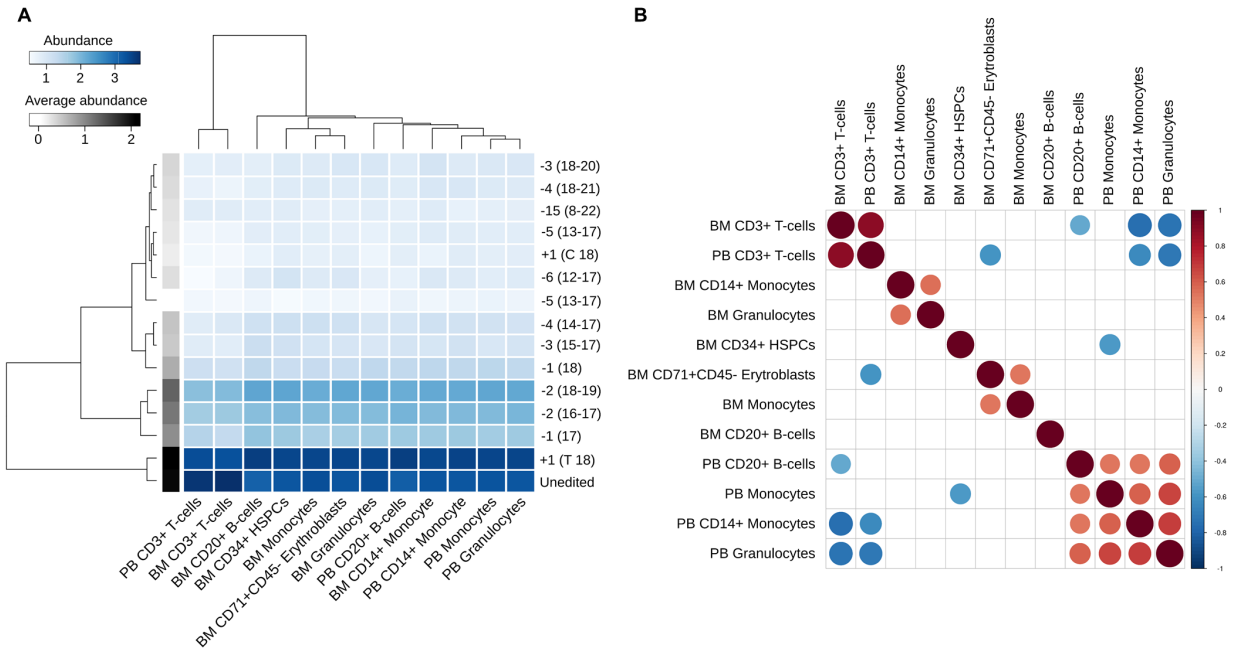

Supplemental Figure 8. Cell lineage gene edit patterns. (A) Heatmap representation of the abundance (log) for the 14 indels with a frequency greater than 1% in at least one lineage plus the unedited allele in BM and PB lineages of ZM17 at 28 weeks post-transplantation. The allele-specific average abundance value (log) is represented by a gray-scale color on the left side of the heatmap. Both columns (lineages) and rows (alleles) are ordered according to their similarity measured by Ward distance. (**B**) The correlation (Pearson's coefficient) among all possible pairs of lineages of ZM17 at 28 weeks post-transplantation based on gene edit distribution. Both circle diameter and color represent Pearson's correlation estimates. Only significant (t-test, alpha = 0.05) correlations are plotted. Columns (and rows) are ordered using Euclidean distance.

Supp 9E. ZM26, *BCL11A* Enhancer

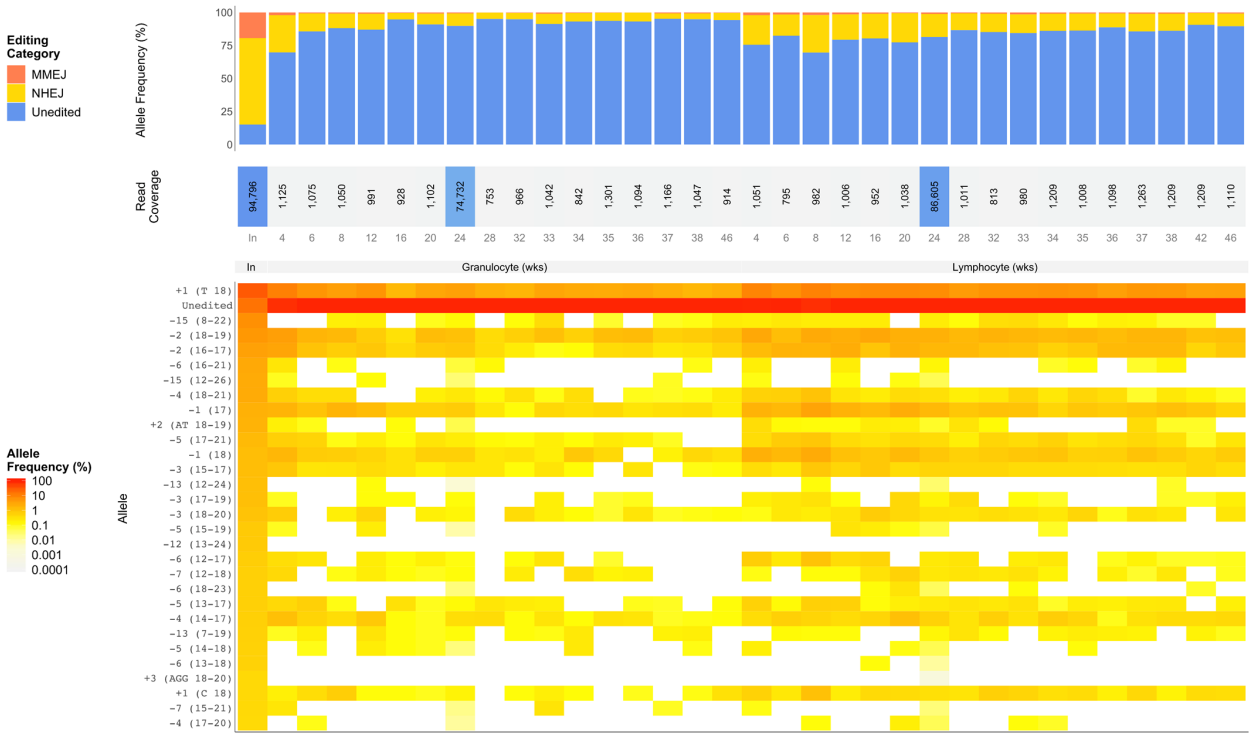

Supp 9B. ZL25, *BCL11A* Enhancer

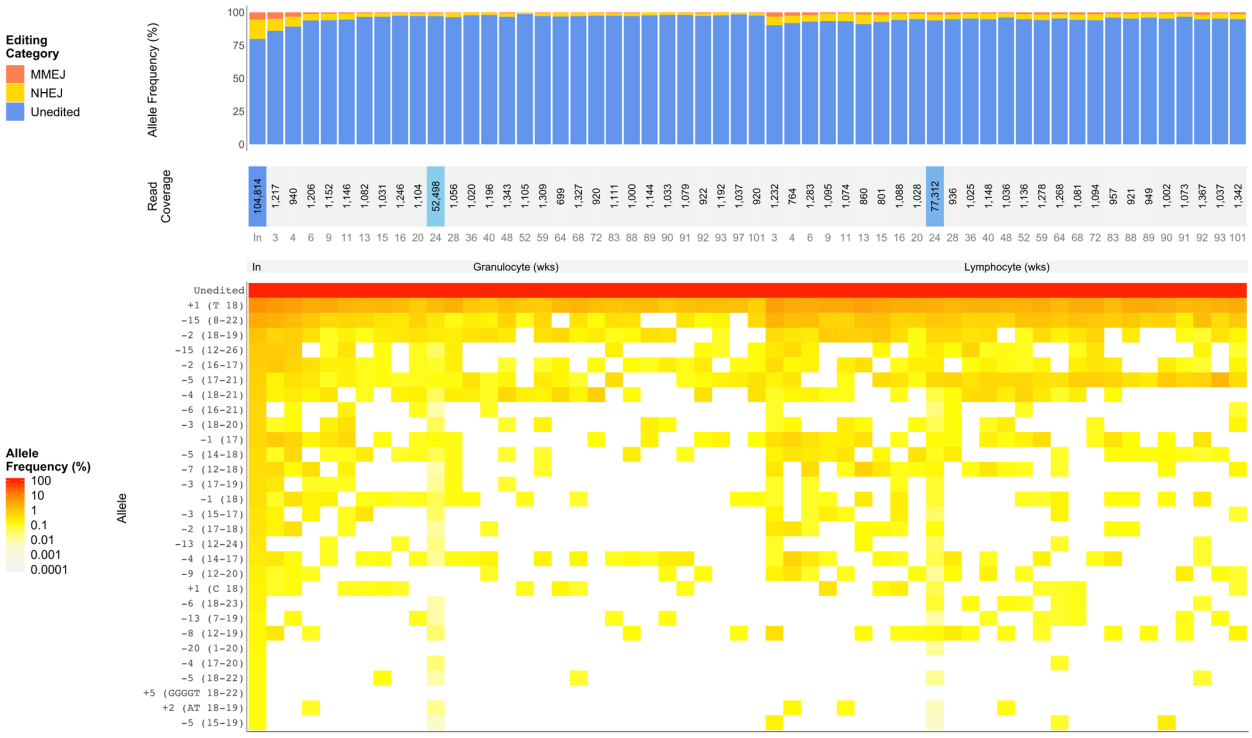

Supp 9C. ZL22, *AAVS1*

Supp 9D. ZL22, *BCL11A* Enhancer

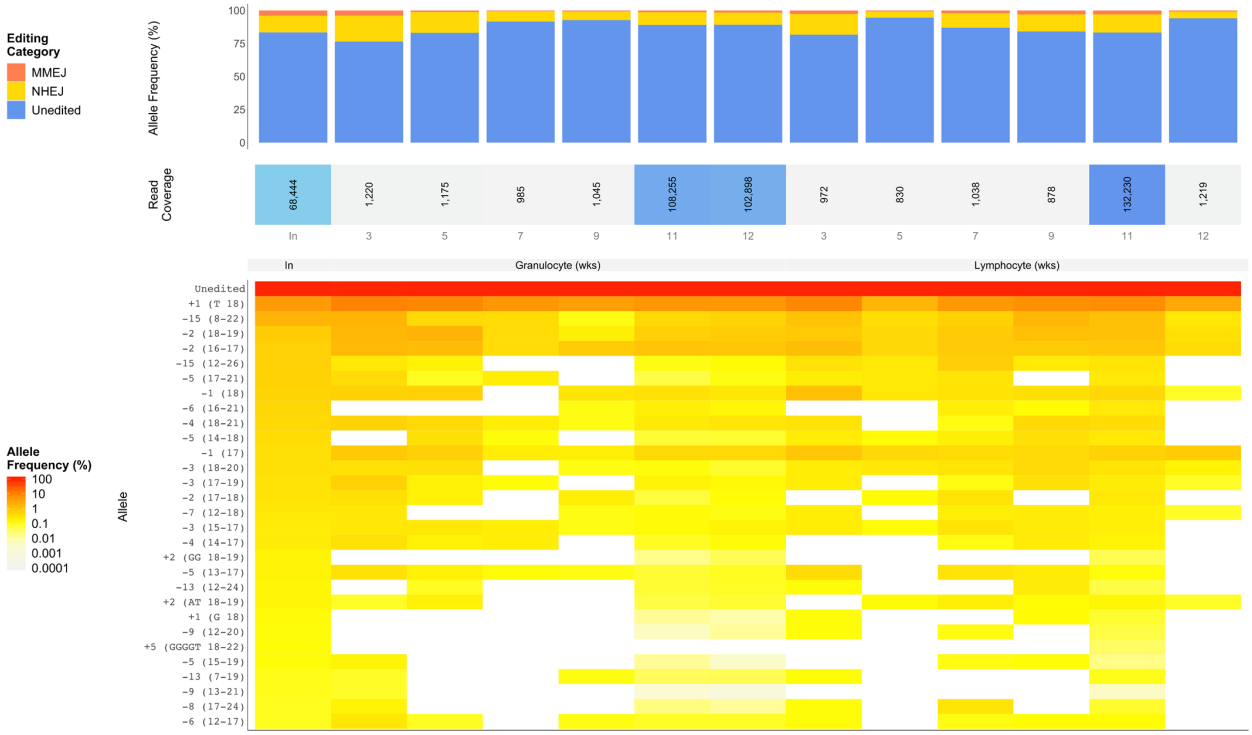

Supp 9E. ZM26, *BCL11A* Enhancer

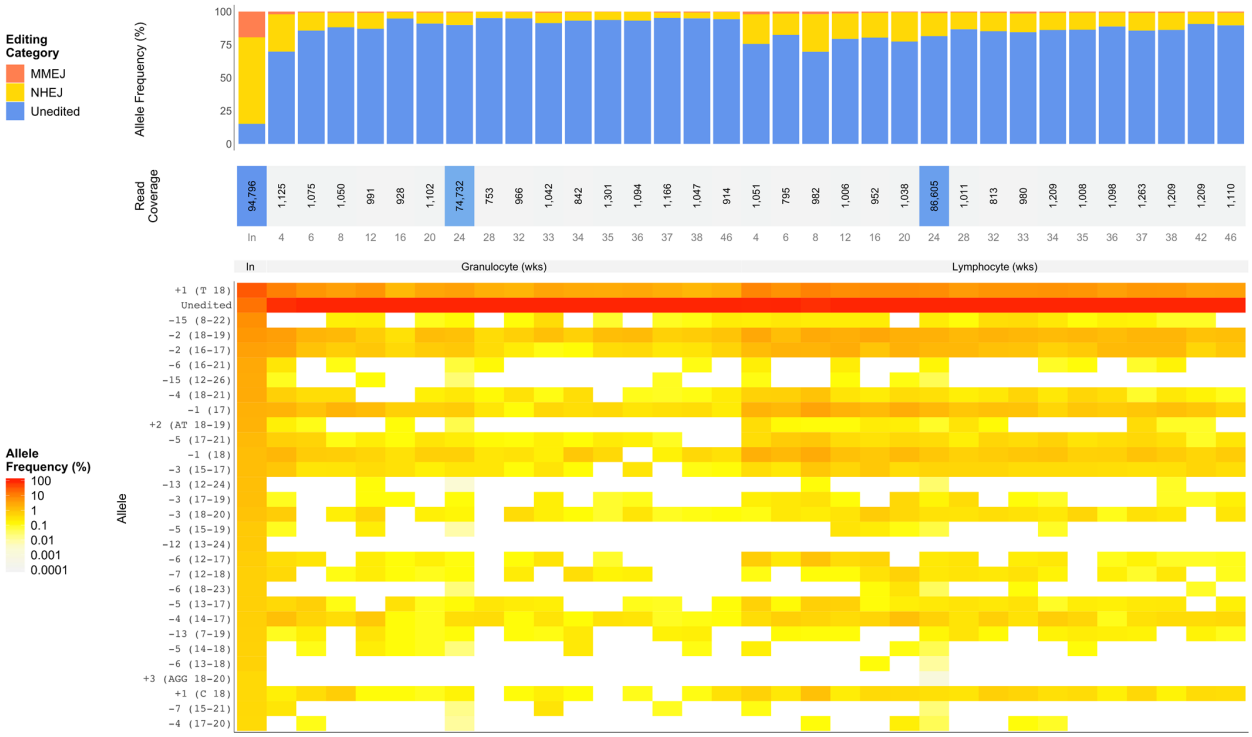

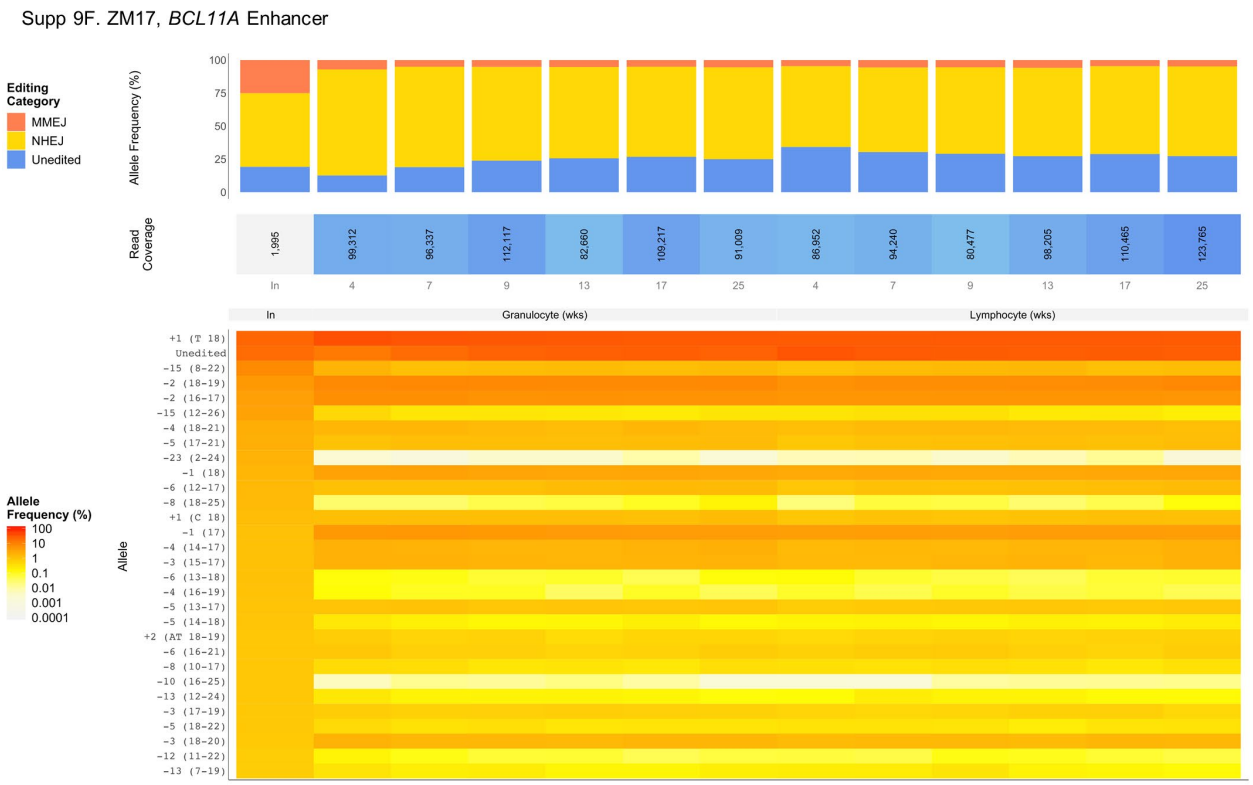

Supplemental Figure 9. Summary of the indel composition in engrafted granulocyte and lymphocyte fractions of peripheral blood over time. Amplicon deep sequencing and analysis was performed to identify (**A**) *AAVS1* edits in ZL25, (**B**) *BCL11A* enhancer edits in ZL25, (**C**) *AAVS1* edits in ZL22, (**D**) *BCL11A* enhancer edits in ZL22, (**E**) *BCL11A* enhancer edits in ZM26, and (**F**) *BCL11A* enhancer edits in ZM17. The 30 alleles with the highest frequency in each sample are shown. In: Infusion product, MMEJ: Microhomology-mediated end joining, NHEJ: Non-homologous end joining. The measured edits in the infusion products for ZL25 and ZL22 were divided by two in these plots to reflect the 1:1 mixing of *AAVS1* and *BCL11A* enhancer edited cells prior to infusion.

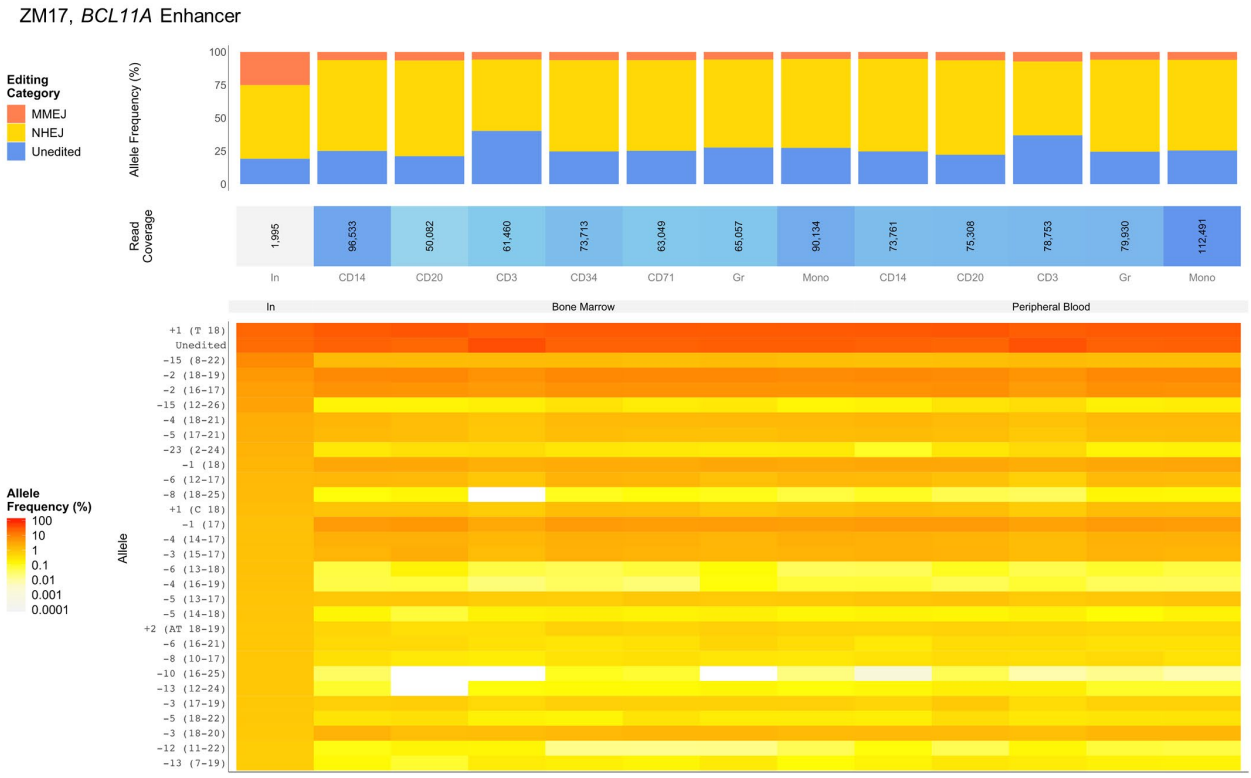

Supplemental Figure 10. Similar indel compositions of *BCL11A* enhancer edits in bone marrow (BM) and peripheral blood (PB) lineages. Amplicon deep sequencing and analysis was performed to identify *BCL11A* enhancer edits in BM (CD14+, CD20+, CD3+, CD34+, CD45-CD71+, granulocyte [Gr] and monocyte [Mono]) and PB (CD14+, CD20+, CD3+, granulocyte [Gr] and monocyte [Mono]) fractions of ZM17 over time. For each fraction, amplicon deep sequencing and indel analysis were performed, and the 30 alleles with the highest frequency are shown. In: Infusion product, MMEJ: Microhomology-mediated end joining, NHEJ: Non-homologous end joining.

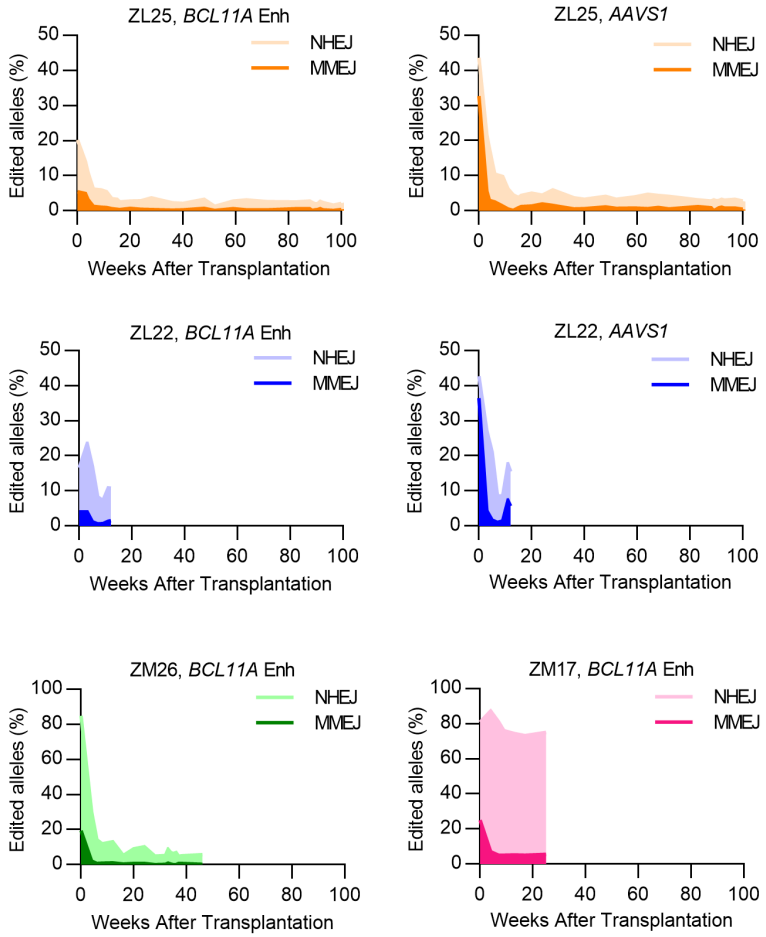

Supplemental Figure 11. Microhomology-mediated end joining (MMEJ) and non-homologous end joining (NHEJ) indel percentages in edited animals over time. Deletions ≥8 bp were categorized as MMEJ, while all other indels were categorized as NHEJ.

Table 1. Summary of gene edited autologous transplantation experiments.

Animal	**ZL25**	**ZL22**	**ZM26**	**ZM17**
Age at transplantation/Sex	4.5/M	5.5/M	4.5/M	4.0/F
Cas9	2×NLS SpCas9	2×NLS SpCas9	3×NLS SpCas9	3×NLS SpCas9
Guide RNA	*AAVS1, BCL11A* enhancer (#1617)	*AAVS1, BCL11A* enhancer (#1617)	*BCL11A* enhancer (#1617)	*BCL11A* enhancer (#1617)
RNP concentration (μM)	10	10	10	10
Apheresis cell number (cells/kg)	3.50×10^6	0.26×10^6 (day 1); 2.53×10^6 (day 2)	2.50×10^6 (day 1); 1.47×10^6 (day 2)	4.12×10^6 (day 1); 6.93×10^6 (day 2)
Electroporation cell concentration (cells/ml)	5.00×10^6	5.00×10^6	1.50×10^6	1.50×10^6
Pre-EP culture time (h)	0	24	24	24
Post-EP culture time (h)	48	48	48	48
Culture plate coating	Retronectin	None	None	None
Infusion product (cells/kg)	0.74×10^6 (*AAVS1*); 0.68×10^6 (*BCL11A* enhancer)	0.58×10^6 (*AAVS1*); 0.65×10^6 (*BCL11A* enhancer)	1.78×10^6	6.06×10^6
Infusion type	Fresh cells	Fresh cells	Cryopreserved cells	Cryopreserved cells
Infusion product indel frequency	73.4% (*AAVS1*); 40.4% (*BCL11A* enhancer)	87.8% (*AAVS1*); 33.2% (*BCL11A* enhancer)	84.9%	80.9%

Note: Indels in the infusion products are measured prior to mixing *AAVS1* and *BCL11A* enhancer edited cells